ORGANOMETALLICS
Organometallics, 1998, 17(17), 3784-3797, DOI:10.1021/om9804226

**Terms & Conditions**

Electronic Supporting Information files are available without a subscription to ACS Web Editions. The American Chemical Society holds a copyright ownership interest in any copyrightable Supporting Information. Files available from the ACS website may be downloaded for personal use only. Users are not otherwise permitted to reproduce, republish, redistribute, or sell any Supporting Information from the ACS website, either in whole or in part, in either machine-readable form or any other form without permission from the American Chemical Society. For permission to reproduce, republish and redistribute this material, requesters must process their own requests via the RightsLink permission system. Information about how to use the RightsLink permission system can be found at http://pubs.acs.org/page/copyright/permissions.html

ACS Publications
MOST TRUSTED. MOST CITED. MOST READ.

Copyright © 1998 American Chemical Society

OM9804226

**Supplementary Material**

M.A. Bennett, M. Bown, D.C.R. Hockless, J.E. McGrady, H.W. Schranz, R. Stranger, and A.C. Willis, Dissociative and non-dissociative pathways in the *endo* to *exo* isomerization of tetramethyl-*o*-xylylene complexes of ruthenium and osmium, $ML_3\{\eta^4\text{-}o\text{-}C_6Me_4(CH_2)_2\}$ {M=Ru, L= $PMe_3$; M=Os, L=$PMe_3$, $PMe_2Ph$}. Formation of Hexamethylbenzene-1,2-diyl complexes by ligand addition to the *exo*- osmium complex, JACS submitted, 1998.

Harold W. Schranz, RSC, ANU, Canberra, ACT 0200, Australia.

**Draft**: Monday, 2 March 1998

## 1. Introduction

This supplementary material describes the application of chemical kinetics theory and simulation to the modelling of the *endo* to *exo* isomerization of the following three tetramethyl-*o*-xylylene complexes of ruthenium and osmium of the form $ML_3\{\eta^4\text{-}o\text{-}C_6Me_4(CH_2)_2\}$ :

(**1**) $Ru(PMe_3)_3\{\eta^4\text{-}o\text{-}C_6Me_4(CH_2)_2\}$
(**2**) $Os(PMe_3)_3\{\eta^4\text{-}o\text{-}C_6Me_4(CH_2)_2\}$
(**3**) $Os(PMe_2Ph)_3\{\eta^4\text{-}o\text{-}C_6Me_4(CH_2)_2\}$

The experimental observations are consistent with exponential decay of the initial reactant species $ML_3\{\eta^4\text{-}endo\text{-}o\text{-}C_6Me_4(CH_2)_2\}$ with an effective unimolecular rate constant $k_{eff}$ which exhibits a dependence on the initial free ligand concentration $[L]_0$. For compounds (**1**) and (**3**) , $k_{eff}$ decreases as $[L]_0$ is raised, whereas for compound (**2**) $k_{eff}$ increases slightly with increasing $[L]_0$.

## 2. Theoretical and Simulation Approach

In the modelling of the isomerization reactions, a combination of theoretical and simulation approaches is employed to extract time-dependent concentrations from the proposed reaction mechanisms. In general, for an arbitrary reaction mechanism, the corresponding system of chemical rate equations is not solvable analytically and numerical and/or approximate solutions must be sought to obtain the detailed time dependences of the concentrations of reactant, intermediate and product species [1]. The goal here is to find the simplest mechanism consistent with the experimental observations of the isomerization kinetics.

The most common method used to solve a system of rate equations is to apply the **steady state approximation (SSA)** [1] to the coupled differential equations obtained from the reaction mechanism. The assumption is made that transient reaction intermediates have very small, stable concentrations so that the time derivative of their concentrations can to be set equal to zero. The concentrations of these intermediate species are expressed in terms of stable reactants and products only. Use of the SSA can place restrictions on the experimental conditions used to study a particular chemical reaction. For example, a vast excess of a reagent may be necessary, or only a small extent of reaction might be allowed. For many chemical reactions steady-state conditions truly exist and the SSA allows valuable mechanistic information to be obtained.

A more general approach for obtaining exact and accurate solutions is that of **numerical simulation** [1-3]. Unlike algebraic approaches, which are often highly simplified, simulations allow detailed models to be developed and tested as data accumulate. Numerical simulation methods generally place few or no constraints on the chemical processes occurring during the reaction and are highly accurate. Two very different computational methods are available:

(1) By far the most commonly used is the **deterministic** approach [1], in which the time-dependence of species concentrations is written as a set of coupled differential equations which are then integrated. The program REACT3 by Whitbeck [2] is employed. It uses Hindmarsh and Cohen's CVODE algorithm for integration of ordinary differential equations [4] and Johnson's implementation of the Hooke-Jeeves simplex algorithm for fitting experimental data [5].

(2) An alternative approach is the **stochastic** method [1,3,6,7], in which changes in a reacting system are modelled by randomly selecting among probability-weighted reaction steps. For chemical reactions whose complex sets of differential equations are difficult to solve - e.g. explosions, nucleation, large ranges of rates or concentrations - it is the method of choice. The program CKS is employed [3].

The methods are completely comparable for non-stiff problems with no partial equilibria. The stochastic method is significantly faster for stiff problems, and the integrator is faster for systems with partial equilibria [3].

The strategy employed here is to use the SSA where possible to obtain expressions for $k_{eff}$ in terms of elementary rate constants and then use the experimental data to provide information on the magnitude of these rate constants. The validity of the SSA in each case is then checked by performing exact (stochastic and deterministic) simulations of the proposed mechanism using rate constants consistent with the experimental data.

## 3. Models

### *3.1 General model*

A general model of competing parallel dissociative and non-dissociative pathways for isomerization of the complexes is provided by the following mechanism:

$$A \underset{\leftarrow}{\rightarrow} B + L \quad (R1)$$

$$B \underset{\leftarrow}{\rightarrow} C \quad (R2)$$

$$C + L \underset{\leftarrow}{\rightarrow} D \quad (R3)$$

$$D + L \underset{\leftarrow}{\rightarrow} E \quad (R4)$$

$$A \underset{\leftarrow}{\rightarrow} D \quad (R5)$$

where:

$A = ML_3\{\eta^4\text{-}endo\text{-}o\text{-}C_6Me_4(CH_2)_2\}$,
$B = ML_2\{\eta^4\text{-}endo\text{-}o\text{-}C_6Me_4(CH_2)_2\}$,
$C = ML_2\{\eta^4\text{-}exo\text{-}o\text{-}(CH_2)_2C_6Me_4\}$,
$D = ML_3\{\eta^4\text{-}exo\text{-}o\text{-}(CH_2)_2C_6Me_4\}$, and
$E = ML_4\{\kappa^2\text{-}o\text{-}(CH_2)_2C_6Me_4\}$.

The corresponding rate equations involve ten rate constants:

$$\frac{d[A]}{dt} = -(k_1 + k_5)[A] + k_{-1}[B][L] + k_{-5}[D]$$

$$\frac{d[B]}{dt} = k_1[A] + k_{-2}[C] - k_{-1}[B][L] - k_2[B]$$

$$\frac{d[C]}{dt} = k_2[B] + k_{-3}[D] - k_{-2}[C] - k_3[C][L]$$

$$\frac{d[D]}{dt} = k_3[C][L] + k_{-4}[E] + k_5[A] - k_{-3}[D] - k_4[D][L] - k_{-5}[D]$$

$$\frac{d[E]}{dt} = k_4[D][L] - k_{-4}[E]$$

$$\frac{d[L]}{dt} = k_1[A] + k_{-3}[D] + k_{-4}[E] - (k_{-1}[B] + k_3[C] + k_4[D])[L]$$

This system is not solvable analytically and appears intractable even with application of the SSA to intermediate concentrations. However, simpler kinetic schemes can be derived by limiting the number of reversible steps. These simpler schemes are then amenable to theoretical solution.

### *3.2 Irreversible model*

The simplest model involves replacing all reversible steps by irreversible steps and requires five elementary rate constants:

$$A \rightarrow B + L \quad (R1)$$

$$B \rightarrow C \quad (R2)$$

$$C + L \rightarrow D \quad (R3)$$

$$D + L \rightarrow E \quad (R4)$$

$$A \rightarrow D \quad (R5)$$

The corresponding rate equations are:

$$\frac{d[A]}{dt} = -(k_1 + k_5)[A]$$

$$\frac{d[B]}{dt} = k_1[A] - k_2[B]$$

$$\frac{d[C]}{dt} = k_2[B] - k_3[C][L]$$

$$\frac{d[D]}{dt} = k_3[C][L] + k_5[A] - k_4[D][L]$$

$$\frac{d[E]}{dt} = k_4[D][L]$$

$$\frac{d[L]}{dt} = k_1[A] - (k_3[C] + k_4[D])[L]$$

and are readily solved for the decay of [A] by direct integration:

$$[A] = [A]_0 \exp[-(k_1 + k_5)t]$$

so that $k_{eff} = k_1 + k_5$ which is independent of [L] in contrast to experiment.

### *3.3 Reversible R1 model*

The next level of sophistication involves including a reversible step for (R1). This makes possible inhibition, caused by high free ligand concentration [L], of the decay of [A] by the dissociative pathway (R1):

$$A \underset{\leftarrow}{\overset{\rightarrow}{}} B + L \qquad (R1)$$

$$B \rightarrow C \qquad (R2)$$

$$C + L \rightarrow D \qquad (R3)$$

$$D + L \rightarrow E \qquad (R4)$$

$$A \rightarrow D \qquad (R5)$$

and yields the following rate equations:

$$\frac{d[A]}{dt} = -(k_1 + k_5)[A] + k_{-1}[B][L]$$

$$\frac{d[B]}{dt} = k_1[A] - k_2[B] - k_{-1}[B][L]$$

$$\frac{d[C]}{dt} = k_2[B] - k_3[C][L]$$

$$\frac{d[D]}{dt} = k_3[C][L] + k_5[A] - k_4[D][L]$$

$$\frac{d[E]}{dt} = k_4[D][L]$$

$$\frac{d[L]}{dt} = k_1[A] - (k_{-1}[B] + k_3[C] + k_4[D])[L]$$

In order to extract the time dependence of [A] it is necessary to apply the SSA approximation to the concentration of [B] which yields:

$$[B] = \frac{k_1[A]}{k_2 + k_{-1}[L]}$$

$$\text{so that } \frac{d[A]}{dt} = -(k_1 + k_5)[A] + k_{-1}[B][L]$$
$$= -k_{eff}[A]$$

and if it is assumed that [L] is small or slowly changing in time, then [A] decays exponentially where $k_{eff} = k_5 + k_1 \left\{\frac{1}{1+k_{-1}[L]/k_2}\right\}$. A further approximation is that the steady state concentration of [L] is near its initial value, $[L] \approx [L]_0$ (valid for excess L). This model exhibits a clear dependence of $k_{eff}$ on [L], with $k_{eff} = k_1 + k_5$ for [L]=0 and $k_{eff} = k_5$ for $[L] \rightarrow \infty$. For a free ligand concentration $[L] = k_2/k_{-1}$, $k_{eff}$ is halfway between these limits. Thus, if this model affords a reasonable description of the experimental behaviour, the rate constants $k_5$ and $k_1$ and the ratio $k_{-1}/k_2$ can be extracted by a fit to experimental data.

## 4. Synthetic Model Calculations: Theory and Simulation

As a test of the theoretical models and approximations developed in section 3 a number of synthetic model calculations were performed. The initial state was such that [A]=1 equivalent and [L]=0, 1, 2, 5, 10, 20 equivalents, and all other initial concentrations are set to zero.

Rate constants for the elementary steps (R1), (R2), (R3) and (R5) were assigned as $k_1=1$, $k_{-1}=10$, $k_2=10$, $k_3=10$, $k_5=2$ and rate constants for step (R4) were chosen from three cases:

(i) reaction (R4) turned **off**: no E species: $k_4=k_{-4}=0$
(ii) reaction (R4) **reversible**: E species in equilibrium with D: $k_4=k_{-4}=10$
(iii) reaction (R4) **irreversible**: E species formed irreversibly from D: $k_4=10$, $k_{-4}=0$

Sample concentration profiles from simulations (CKS) are shown in Figs. 1-3 for reaction (R4) turned off (case (i)) with [L]0=0, 1, and 10 equivalents, respectively. The decay of A is essentially exponential to high accuracy and is consistent with the SSA calculation of $k_{eff}$ (superimposed in Figs. 1-3 on the simulation decay), i.e.

$$k_{eff,SSA} = k_5 + k_1 \left\{\frac{1}{1+k_{-1}[L]/k_2}\right\} = 2 + 1 \left\{\frac{1}{1+[L]}\right\} \quad .$$

The effect of the introduction of reaction (R4) in a reversible sense (case(ii)) is compared with the absence of reaction (R4) (case(i)) in Figs. 4, 5, and 6 for the time dependence of the A, D and E species for [L]=0, 1 and 10 equivalents, respectively. The decay of the A species is still exponential and does not seem to be significantly affected by reaction (R4).

Exponential fits were made to the decay of [A] with time to yield $k_{eff}$ and compared to the SSA predictions of the Reversible R1 model (section 3.3) in Fig 7 and in the following table:

| Reaction (R4) | $[L]_0$ | Calculation SSA Reversible R1 model (section 3.3) | Simulation CKS | Simulation REACT |
|---|---|---|---|---|
| off | 0 | 3.000 | 2.881±0.003 | 2.886±0.004 |
| | 1 | 2.500 | 2.454±0.006 | 2.459±0.005 |
| | 5 | 2.167 | 2.142±0.010 | 2.147±0.002 |
| | 10 | 2.091 | 2.114±0.017 | 2.080±0.001 |
| | 20 | 2.048 | 2.077±0.040 | 2.041±0.001 |
| | ∞ | 2.000 | | |
| reversible | 0 | 3.000 | 2.912±0.002 | 2.890±0.003 |
| | 1 | 2.500 | 2.488±0.002 | 2.518±0.003 |
| | 5 | 2.167 | 2.148±0.004 | 2.160±0.002 |
| | 10 | 2.091 | 2.071±0.006 | 2.084±0.001 |
| | 20 | 2.048 | 1.925±0.003 | 2.043±0.001 |
| | ∞ | 2.000 | | |
| irreversible | 0 | 3.000 | 2.908±0.002 | 2.920±0.002 |
| | 1 | 2.500 | 2.537±0.006 | 2.582±0.005 |
| | 5 | 2.167 | 2.138±0.009 | 2.163±0.002 |
| | 10 | 2.091 | 2.038±0.017 | 2.084±0.001 |
| | 20 | 2.048 | 2.161±0.023 | 2.043±0.001 |
| | ∞ | 2.000 | | |

Kinetic parameters extracted from simulations are compared with the SSA model:

| Reaction (R4) | Item | Calculation SSA Reversible R1 model (section 3.3) | Simulation CKS | Simulation REACT |
|---|---|---|---|---|
| off | $k_5$ | 2 | 2.031±0.018 | 1.991±0.005 |
| | $k_1$ | 1 | 0.852±0.026 | 0.876±0.007 |
| | $k_{-1}/k_2$ | 1 | 1.055±0.133 | 0.881±0.027 |
| reversible | $k_5$ | 2 | 1.896±0.048 | 1.973±0.014 |
| | $k_1$ | 1 | 1.011±0.060 | 0.919±0.018 |
| | $k_{-1}/k_2$ | 1 | 0.652±0.162 | 0.713±0.058 |
| irreversible | $k_5$ | 2 | 2.019±0.089 | 1.947±0.034 |
| | $k_1$ | 1 | 0.897±0.122 | 0.980±0.041 |
| | $k_{-1}/k_2$ | 1 | 0.870±0.489 | 0.593±0.103 |

The SSA model appears to yield a reasonable prediction of the [L] dependence of $k_{eff}$, even for [L]=0 where the SSA assumption on [B] and the assumption that $[L]=[L]_0$ is least accurate. The agreement between the simulation results (CKS, REACT) and the SSA predictions in Fig. 7 is surprisingly good. The errors in the CKS simulation results are larger than for the REACT simulation results, a consequence of the noise in the Monte Carlo sampling used in the former and the deterministic algorithm used in the latter.

The effective rate constant $k_{eff}$ and the extracted kinetic parameters are insensitive to the presence or absence of reaction 4. No clear trend is apparent. Noise present in the simulation data and the few (5) data points used in the fit may account for most of the variation in the fitted kinetic parameters.

Given the success above, it appears justified to employ the SSA model to extract some kinetic parameters from the experimental data: the rate constants $k_5$ and $k_1$ and the ratio $k_{-1}/k_2$. The remaining rate constants are unknown and are assumed to be fast, and are given arbitrarily large values. It is not known whether changing these values would have any effect on the decay of A. If they are sufficiently fast it is unlikely that they would represent a bottleneck to reaction and thus the experimental results might be insensitive to their actual values. This could be checked by performing a wider variety of simulations and varying the magnitude of the rate constants, performing essentially a sensitivity analysis for the effect on the concentration dependence of A.

## 5. Isomerization of compound (1) $Ru(PMe_3)_3\{\eta^4$- *endo* -*o*-$C_6Me_4(CH_2)_2\}$

### *5.1 Free ligand dependence and fits of the SSA model*

Experimental results for the dependence of $k_{eff}$ on the initial amount of free ligand $[L]_0$ at a temperature of 357.5K were used to fit to the **SSA Reversible R1 model** (section 3.3) yielding (see Fig. 8):

$k_5 = (1.78\pm0.62)\times10^{-5}\ s^{-1}$
$k_1 = (6.56\pm0.86)\times10^{-5}\ s^{-1}$
$k_{-1}/k_2 = (0.95\pm0.44)$ equivalent$^{-1}$
(Regression Coefficient=0.968)

In terms of the **SSA Reversible R1 model** (section 3.3), these kinetic parameters can be interpreted to mean that the first step in the dissociative pathway (R1) is 3.7 times as fast as the dissociative pathway (R5). The effective rate constant for the decay of A is predicted to range from $k_{eff} = 8.34\times10^{-5}\ s^{-1}$ at $[L]_0=0$ to $k_{eff} = 1.78\times10^{-5}\ s^{-1}$ at $[L]_0=\infty$, which is in reasonable agreement (13% average relative deviation) with the original experimental data. The worst agreement is for a single point at the highest $[L]_0$ concentration (31%) and agreement would be far better if this point were discarded. It is unknown if the high value of this point is a real effect (acceleration of the rate constant by some arbitrarily large excess of ligand seems unlikely) or experimental error. The fitted ratio of $k_{-1}/k_2 = 0.95$ equivalent$^{-1}$ can be interpreted to mean that for an initial ligand concentration of $[L] = k_2/k_{-1} = 1.05$ equivalents the effective rate constant $k_{eff}$ is halfway between its value at the [L]=0 and $[L]=\infty$ limits.

### *5.2 Simulation of the free ligand dependence*

In order to perform simulations, the **SSA Reversible R1 model** (section 3.3) was adopted and rate constants were chosen consistent with the derived parameters - only the ratio of $k_{-1}/k_2$ is known - and for unknown rate constants a value of 10 was chosen. Thus:

$$k_1=6.6\times10^{-5}\ s^{-1},$$
$$k_{-1}=9.5\times10^{-5}\ s^{-1}\ \text{equivalent}^{-1},$$
$$k_2=10\times10^{-5}\ s^{-1},$$
$$k_3=10\times10^{-5}\ s^{-1},$$
$$k_5=1.8\times10^{-5}\ s^{-1}$$

and all other rate constants were set to zero. Thus step (R4) was eliminated by choosing $k_4=k_{-4}=0$ (case(i)). This set of rate constants is one of a family of sets of rate constants that would be consistent with the observed behaviour. Thus, without further experimental data (or *ab initio* information) it is not possible to make quantitative conclusions about the rate of appearance of intermediates and products, only about the disappearance of the reactant molecule. Typical (CKS) simulations are shown in Figs. 9, 10 and 11 for $[L]_0=0$, 1 and 10 equivalents, respectively.

General observations:

- The simulated decay of reactant A is exponential and consistent with the SSA calculation based on the assigned rate constants:.

$$k_{eff,SSA} = k_5 + k_1\left\{\frac{1}{1+k_{-1}[L]/k_2}\right\} = \left[1.8 + 6.6\left\{\frac{1}{1+0.95\ [L]}\right\}\right]\times10^{-5}\ s^{-1}$$

- The level of intermediate concentrations is suppressed by excess of free ligand L.
- The level of ligand concentration [L] is (unsurprisingly) stable for excess of ligand.

Effective rate constants are extracted from (CKS, REACT) simulations and compared with the experiment and SSA predictions in Fig. 12 and in the table:

| $[L]_0$ equivalents | rate ($10^{-5}$ $s^{-1}$) experiment | error ($10^{-5}$ $s^{-1}$) experiment | rate ($10^{-5}$ $s^{-1}$) calculated SSA | rate ($10^{-5}$ $s^{-1}$) simulated CKS | error ($10^{-5}$ $s^{-1}$) simulated CKS | rate ($10^{-5}$ $s^{-1}$) simulated REACT | error ($10^{-5}$ $s^{-1}$) simulated REACT |
|---|---|---|---|---|---|---|---|
| 0.0000 | 8.0390 | 0.45900 | 8.3351 | 6.6036 | 0.0188 | 6.6070 | 0.0640 |
| 0.12500 | | | 7.6362 | | | | |
| 0.25000 | | | 7.0719 | | | | |
| 0.50000 | 7.2090 | 0.28800 | 6.2167 | | | 5.4547 | 0.0626 |
| 1.0000 | 4.6600 | 0.30800 | 5.1328 | 4.6008 | 0.0165 | 4.6670 | 0.0558 |
| 2.0000 | 3.8820 | 0.27300 | 4.0319 | | | 3.7440 | 0.0414 |
| 5.0000 | 2.3280 | 0.14600 | 2.9135 | | | 2.7627 | 0.0197 |
| 10.000 | 2.2600 | 0.11300 | 2.3993 | 2.3012 | 0.0028 | 2.3170 | 0.0096 |
| 20.000 | 2.7550 | 0.13000 | 2.1038 | 2.0369 | 0.0027 | 2.0615 | 0.0046 |

Agreement is reasonable with largest deviations occurring between the simulations and the experiment at the highest ([L]=20 equivalents) and lowest ([L]=0 equivalents). The former (25%) deviation is due to the bad fit of the SSA model used to extract the kinetic parameters used in the simulations and the latter (18%) deviation is possibly due to the partial breakdown of the SSA model for low ligand concentrations (when intermediate concentrations are highest).

## 6. Isomerization of compound (3) $Os(PMe_2Ph)_3\{\eta^4$- *endo* -*o*-$C_6Me_4(CH_2)_2\}$

### *6.1 Free ligand dependence and fits of the SSA model*

A similar fit of kinetic parameters was performed for compound (**3**). Experimental results for the dependence of $k_{eff}$ on the initial amount of free ligand $[L]_0$ were used to fit to the **SSA Reversible R1 model** (section 3.3) yielding (Fig. 13):

$k_5 = (3.04\pm0.13)\times10^{-5}$ $s^{-1}$

$k_1 = (1.27\pm0.17)\times10^{-5}$ $s^{-1}$

$k_{-1}/k_2 = (0.83\pm0.39)$ $equivalent^{-1}$

(Regression Coefficient=0.967)

Similar interpretation of these parameters exist as for the Ru isomerization (compound (**1**)). The fitted ratio of $k_{-1}/k_2 = 0.83$ $equivalent^{-1}$ can be interpreted to mean that for an initial ligand concentration of $[L] = k_2/k_{-1} = 1.20$ equivalents the effective rate constant $k_{eff}$ is halfway between its value at the [L]=0 and [L]=∞ limits.

The neglect of the reversible formation of the species E from species D may be an issue. However, the synthetic simulations in section 4.1 indicated no significant dependence of the decay of the reactant A upon the presence or absence of step (R4). Whether this changes for a mechanism which involves more reversible steps remains an open question.

A reasonable interpretation of the lower dependence of $k_{eff}$ on [L] is that the nondissociative mechanism (R5) is relatively more important for the isomerization of compound (**3**) than for the isomerization of compound (**1**). Similar simulations could also be performed as for the compound (**1**) system. The sensitivity of the decay of the reactant A to the presence of step (R4) could be tested by including this step with different rate constants.

## 7. Isomerization of compound (2) $Os(PMe_3)_3\{\eta^4$- *endo* -*o*-$C_6Me_4(CH_2)_2\}$

### *7.1 Free ligand dependence and SSA model fit*

The experimental observations are consistent with exponential decay of the initial reactant species compound (**2**) with an effective unimolecular rate constant $k_{eff}$ which exhibits a dependence on the initial free ligand concentration $[L]_0$ where the ligand L=$PMe_3$.

Unlike previous systems, where $k_{eff}$ decreases significantly as $[L]_0$ is raised, for this system $k_{eff}$ increases slightly as $[L]_0$ is raised. The dependence of the isomerization of compound (**2**) upon the initial free ligand concentration $[L]_0$ is distinctly different from that of the other two experimental systems and the fit shown in Fig. 14 is probably meaningless in terms of kinetic parameters. The fit does show that the point halfway between the [L]=0 and [L]=∞ limits is reached for [L] = 1/1.80 = 0.56 equivalents.

One explanation is that this experiment is showing little or no dependence of $k_{eff}$ on [L] so that it is really a case where all the steps are irreversible (section 3.2) so that

$k_{eff} = k_1 + k_5$ which is independent of [L]. Of course the individual contributions of the two pathways cannot be separated from the data.

A second explanation is that about 1 equivalent of ligand is being used to accelerate the decay of A, perhaps due to extra reversible steps not included in the **R1 reversible mechanism** (section 3.3). What steps this may involve is likely to be any of the steps involving ligand uptake, (R1), (R3), (R4).

Since it is the reversible dissociative mechanism that allows a decrease of $k_{eff}$ with the amount of free ligand [L] it is likely that this mechanism does not play a major role for this system. Thus, a subset of the general model including only the nondissociative pathways is likely to be a good description. In section 7.2 a reaction scheme is described which incorporates only reactions (R4) and (R5) of the general model in section 3.1.

### *7.2 Reversible R5 model*

A subset of the general model which includes a reversible step for (R5) in competition with an irreversible step for (R4), allows us to observe mild enhancement caused by high free ligand concentration [L] of the decay of [A] by the nondissociative pathway:

$$A \underset{\leftarrow}{\overset{\rightarrow}{}} D \qquad (R5)$$

$$D + L \rightarrow E \qquad (R4)$$

yielding the rate equations:

$$\frac{d[A]}{dt} = -k_5[A] + k_{-5}[D]$$

$$\frac{d[D]}{dt} = k_5[A] - k_{-5}[D] - k_4[D][L]$$

$$\frac{d[E]}{dt} = k_4[D][L]$$

$$\frac{d[L]}{dt} = -k_4[D][L]$$

In order to extract the approximate time dependence of [A] it is necessary to apply the SSA approximation to the concentration of [D] which yields

$$[D] = \frac{k_5[A]}{k_{-5} + k_4[L]}$$

and if it is assumed that [L] is small or slowly changing in time then

$$\frac{d[A]}{dt} = -k_{eff}[A] \text{ where } k_{eff} = \left\{\frac{k_5}{1+k_{-5}/k_4[L]}\right\}.$$

A further approximation is that the steady state concentration of [L] is near its initial value, $[L] \approx [L]_0$ (valid for excess L). This, model exhibits a clear dependence of $k_{eff}$ on [L], with $k_{eff} = 0$ for [L]=0 and $k_{eff} = k_5$ for $[L] \rightarrow \infty$. For a free ligand concentration $[L] = k_{-5}/k_4$, $k_{eff}$ is halfway between these limits. Thus, if this model affords a reasonable description of the experimental behaviour, the rate constants $k_5$ and the ratio $k_{-5}/k_4$ can be extracted by a fit.

Some caution is required as the assumptions made are likely to be only valid for sufficiently high initial ligand concentration, $[L]_0 >> 1$. For example the above

expression for $k_{eff}=0$ for $[L]_0=0$ whereas simulation results of the model indicate a finite value for $k_{eff}$. Thus, a better treatment is afforded by exact simulation of the reversible R5 model.

### *7.3 Application of the reversible R5 model to experiment*

As a test of the theoretical models and approximations developed in section 7.2 a fit was made to the expression for $k_{eff}$ as a function of $[L]_0$ as shown in Fig. 15. Because of the approximations made in deriving this expression and the errors apparent in the experimental points, the fitted values were only used as a rough guide. The fitted parameters are identical whether the [L]=0 point is included or excluded. It was included in the fit in Fig. 15 and the following errors and regression coefficient are obtained if it is excluded (the approximate functional form has $k_{eff}=0$ for [L]=0 ):

$k_5 = (1.144\pm0.021)\times10^{-4}\ s^{-1}$

$k_{-5}/k_4 = (0.0437\pm0.0377)$ equivalent$^{-1}$

(Regression Coefficient=0.567)

These values were used in initial simulations and modifications were found to be necessary to accommodate a good fit. For the final simulations, the following values allowed for a reasonable representation of the results.

$k_5 = 1.144\times10^{-4}\ s^{-1}$

$k_{-5} = 0.0487\times10^{-4}\ s^{-1}$

$k_4 = 0.59268\times10^{-4}\ s^{-1}$equivalent$^{-1}$

$k_{-5}/k_4 = 0.08217$ equivalent

The decay of the reactant, A, is plotted in Fig. 16, with exponential fits, for different initial concentrations $[L]_0$=0,1,2,3,4,5,10,15,20 equivalents. A slight plateau is evident at longer times for $[L]_0=0$ (≈4% of initial A at 13.9 hours) and $[L]_0=1$ (≈2% of initial A at 13.9 hours). This region is near the limits of experimental accessibility (≈1% of initial A). Indeed, the corresponding experiments may not have been run to completion (≈11-12 hours for 1% of A remaining given $k_{eff} = 1.1\times10^{-4}\ s^{-1}$).

Examples of simulated concentration profiles for A,D, E and L are shown in Figs. 17-20 for $[L]_0$=0,1,2,20 equivalents, respectively. These plots show that the steady state approximation for D is poor for [L]=0,1,2 equivalents but is probably quite reasonable for [L]=20 equivalents.

The comparison between the experimental and simulation dependence of $k_{eff}$ with $[L]_0$ is given in the following table and Fig. 21 together with fits to the approximate expression. The simulation predictions appear to be a reasonable model of the experimental trend. The simulated and experimental shape of $k_{eff}$ vs [L] is somewhat different from the approximate prediction (fitted solid and dashed curve), especially for low [L] as expected from the breakdown of the approximations made.

Comparison between the experimental and simulation dependence of $k_{eff}$ with $[L]_0$ for the reaction of the $Os(PMe_3)_3$ system.

| $[L]_0$/equivalents | Experiment $k_{eff}/(10^{-4}\ s^{-1})$ | Experiment error/$(10^{-4}\ s^{-1})$ | Simulation $k_{eff}/(10^{-4}\ s^{-1})$ |
|---|---|---|---|
| 0 | 1.0070 | 0.0232 | 1.0071 |
| 1 | 1.0981 | 0.0215 | 1.0633 |
| 2 | 1.1145 | 0.0230 | 1.0922 |
| 3 | | | 1.1074 |
| 4 | 1.1446 | 0.0230 | 1.1162 |
| 5 | | | 1.1218 |
| 10 | 1.0977 | 0.0215 | 1.1333 |
| 15 | | | 1.1371 |
| 20 | 1.1731 | 0.0231 | 1.1389 |

## 8. Concluding Comments

Analysis of the three isomerization systems has been performed in terms of simple chemical kinetic models with parallel dissociative and nondissociative pathways. Good agreement is obtained for the *endo-* to *exo-* isomerization of the compounds (**1**) and (**3**) using a model with a reversible first step in the dissociative pathway. The isomerization of compound (**2**) did not follow this behaviour and instead was successfully described by a related model using a reversible nondissociative pathway.

An interesting issue is that of temperature dependence. If the key elementary steps involved have different temperature dependences (energetics i.e. barrier heights, entropic factors) then it is possible that a cross-over between the nondissociative pathway and the dissociative pathway can occur as a function of temperature. For example, if one pathway had a low barrier height and large entropy and the other had the reverse, the former pathway would be important at low temperatures and the latter would be important at high temperatures. This crossover could also be modelled given further data on the temperature dependence of $k_{eff}$.

## References


[1] J. I. Steinfeld, J. S. Francisco, and W. L. Hase, Chemical Kinetics and Dynamics (Prentice-Hall, New Jersey, 1989).

[2] Whitbeck, M., 1992, Numerical Modeling of Chemical Reaction Mechanisms, Tetrahedron Computer Methodology, Vol 3, No. 6B, pp 497-505.

[3] CKS, B. Hinsberg and F. A. Houle, IBM Research Division, Almaden Research Center, San Jose, California 95120-6099, U.S.A.

[4] Scott D. Cohen and Alan C. Hindmarsh, CVODE User Guide, LLNL Report UCRL-MA-118618, September 1994.

[5] R. Hooke and T. A. Jeeves, "Direct Search Solution of Numerical and Statistical Problems", Journal of the ACM, Vol.8 pp. 212-229, April 1961; by Arthur F. Kaupe Jr., Communications of the ACM, Vol 6. p.313 (June 1963).

[6] D. L. Bunker, B. Garrett, T. Kliendienst and G.S. Long III, Combustion and Flame, Vol 23, p 373 (1974).

[7] D. T. Gillespie, Journal of Computational Physics, Vol 22, p 403 (1976).

# Fig. 1. Synthetic Model Simulation (CKS): (R4) off, $[L_0] = 0$

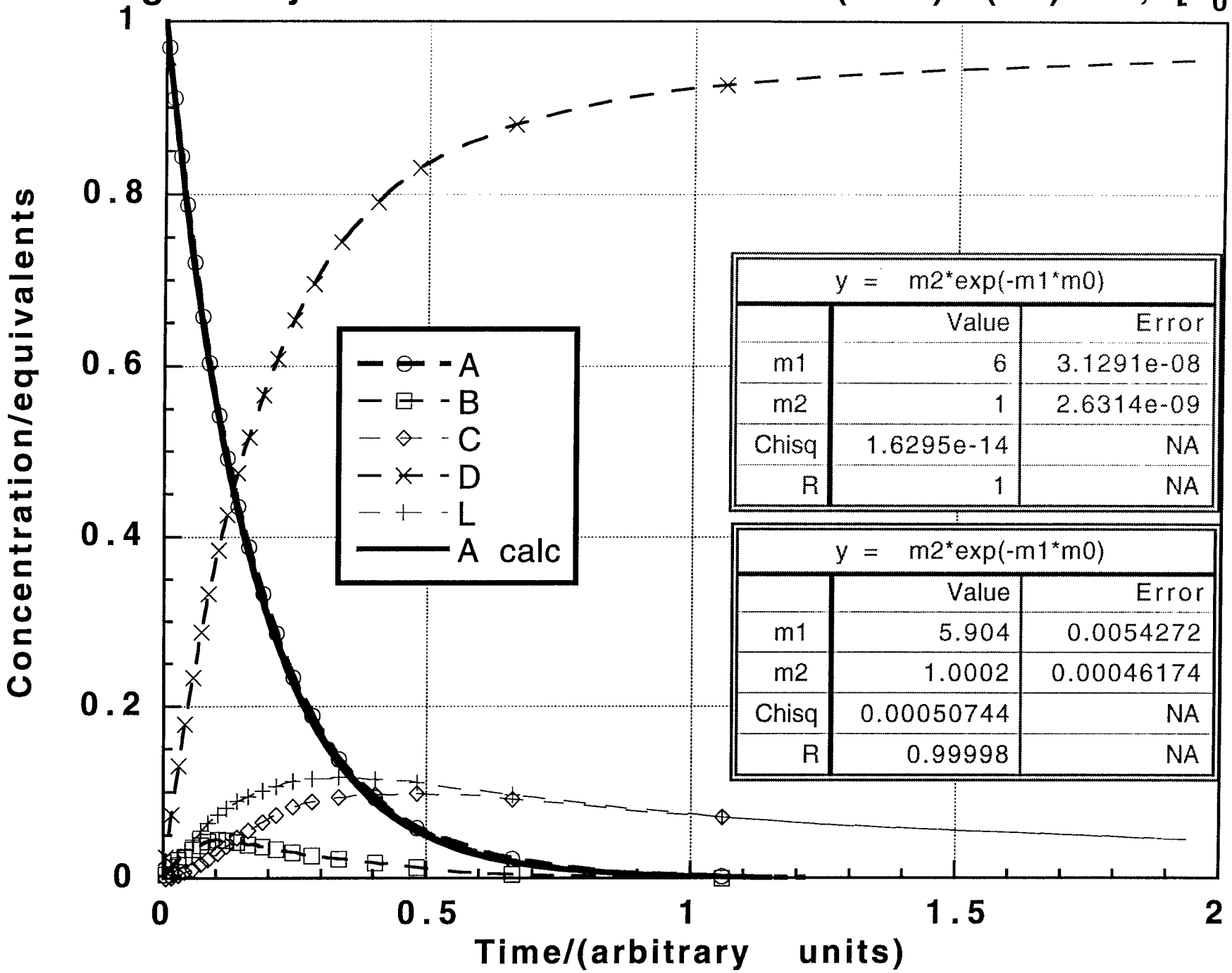


| y = m2*exp(-m1*m0) | | |
|---|---|---|
| | Value | Error |
| m1 | 6 | 3.1291e-08 |
| m2 | 1 | 2.6314e-09 |
| Chisq | 1.6295e-14 | NA |
| R | 1 | NA |

| y = m2*exp(-m1*m0) | | |
|---|---|---|
| | Value | Error |
| m1 | 5.904 | 0.0054272 |
| m2 | 1.0002 | 0.00046174 |
| Chisq | 0.00050744 | NA |
| R | 0.99998 | NA |

# Fig. 2. Synthetic Model Simulation (CKS): (R4) off, $[L_0] = 1$

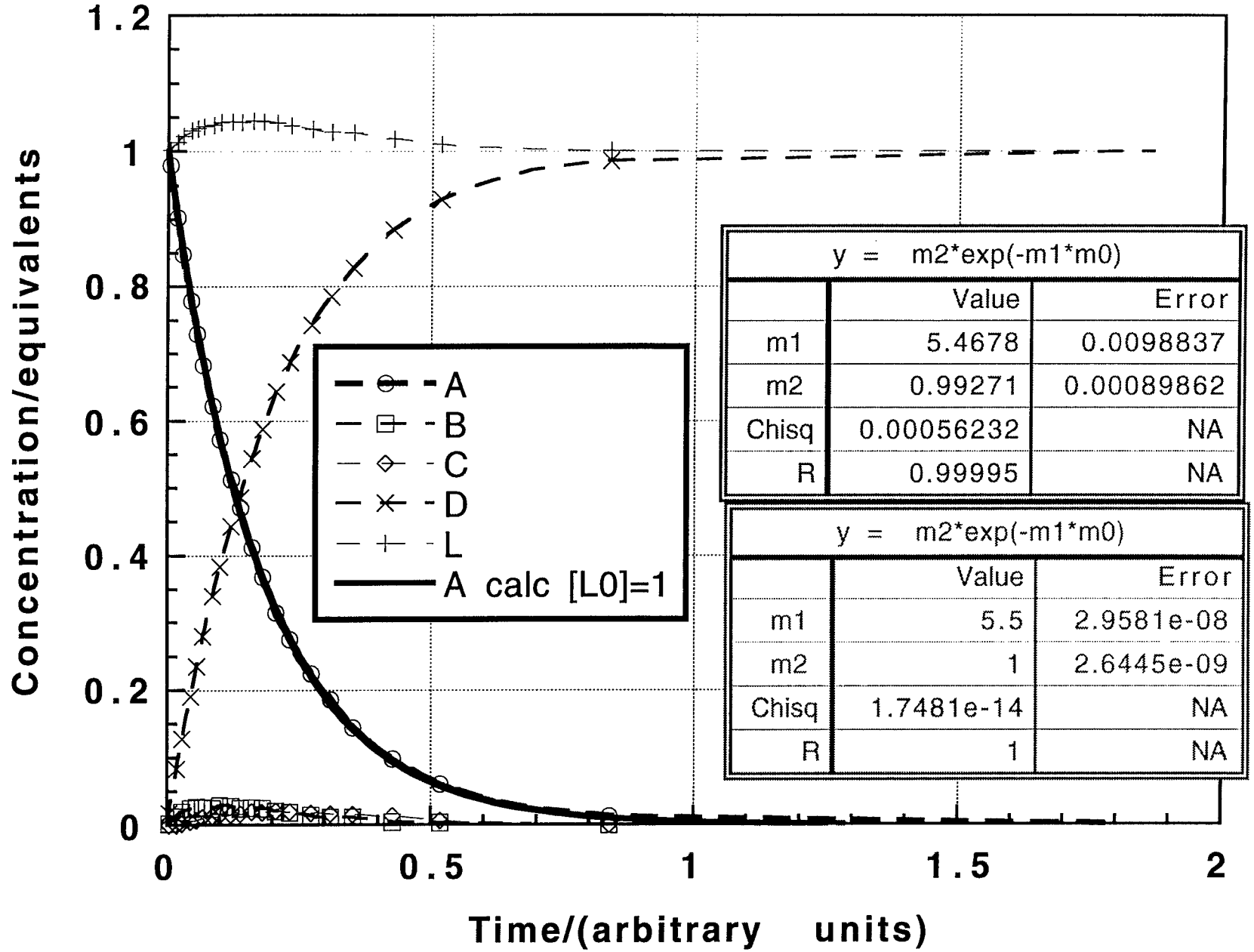

# Fig. 3. Synthetic Model Simulation (CKS): (R4) off, $[L_0] = 10$

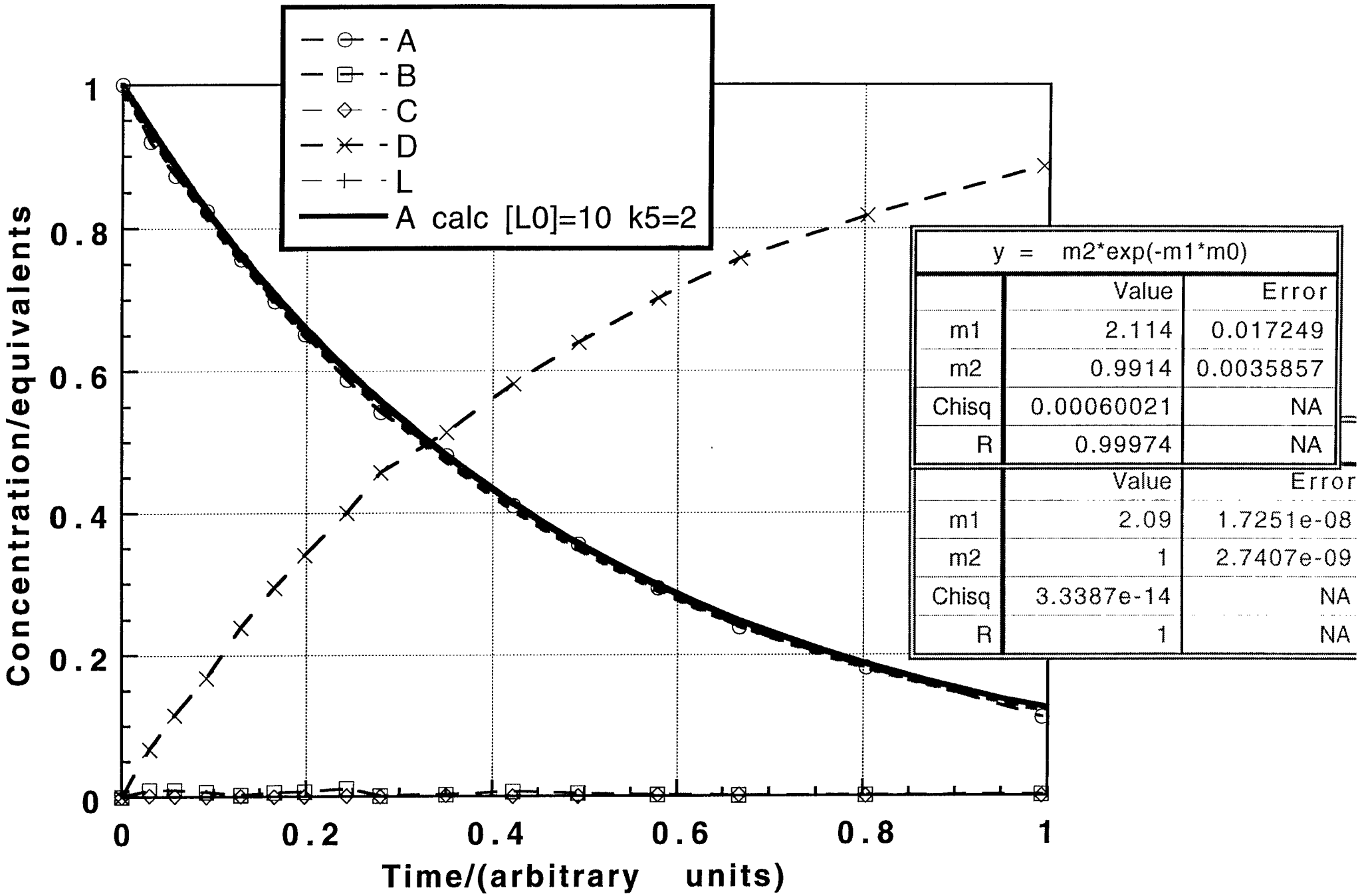


| y = m2*exp(-m1*m0) | | |
|---|---|---|
| | Value | Error |
| m1 | 2.114 | 0.017249 |
| m2 | 0.9914 | 0.0035857 |
| Chisq | 0.00060021 | NA |
| R | 0.99974 | NA |

| | Value | Error |
|---|---|---|
| m1 | 2.09 | 1.7251e-08 |
| m2 | 1 | 2.7407e-09 |
| Chisq | 3.3387e-14 | NA |
| R | 1 | NA |

# Fig. 4. Synthetic Model Simulation (CKS): $[L_0] = 0$

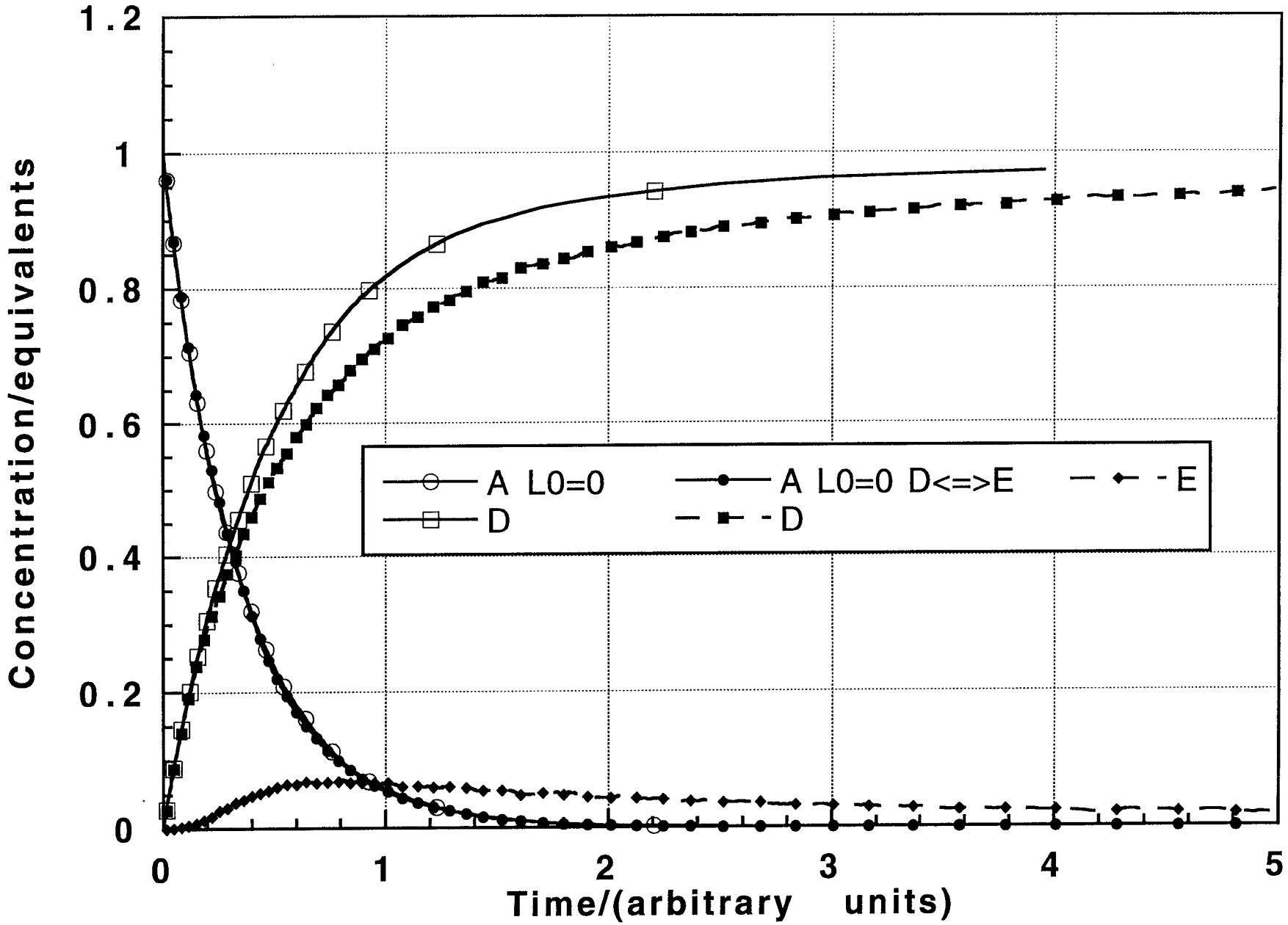

# Fig. 5. Synthetic Model Simulation (CKS): $[L_0] = 1$

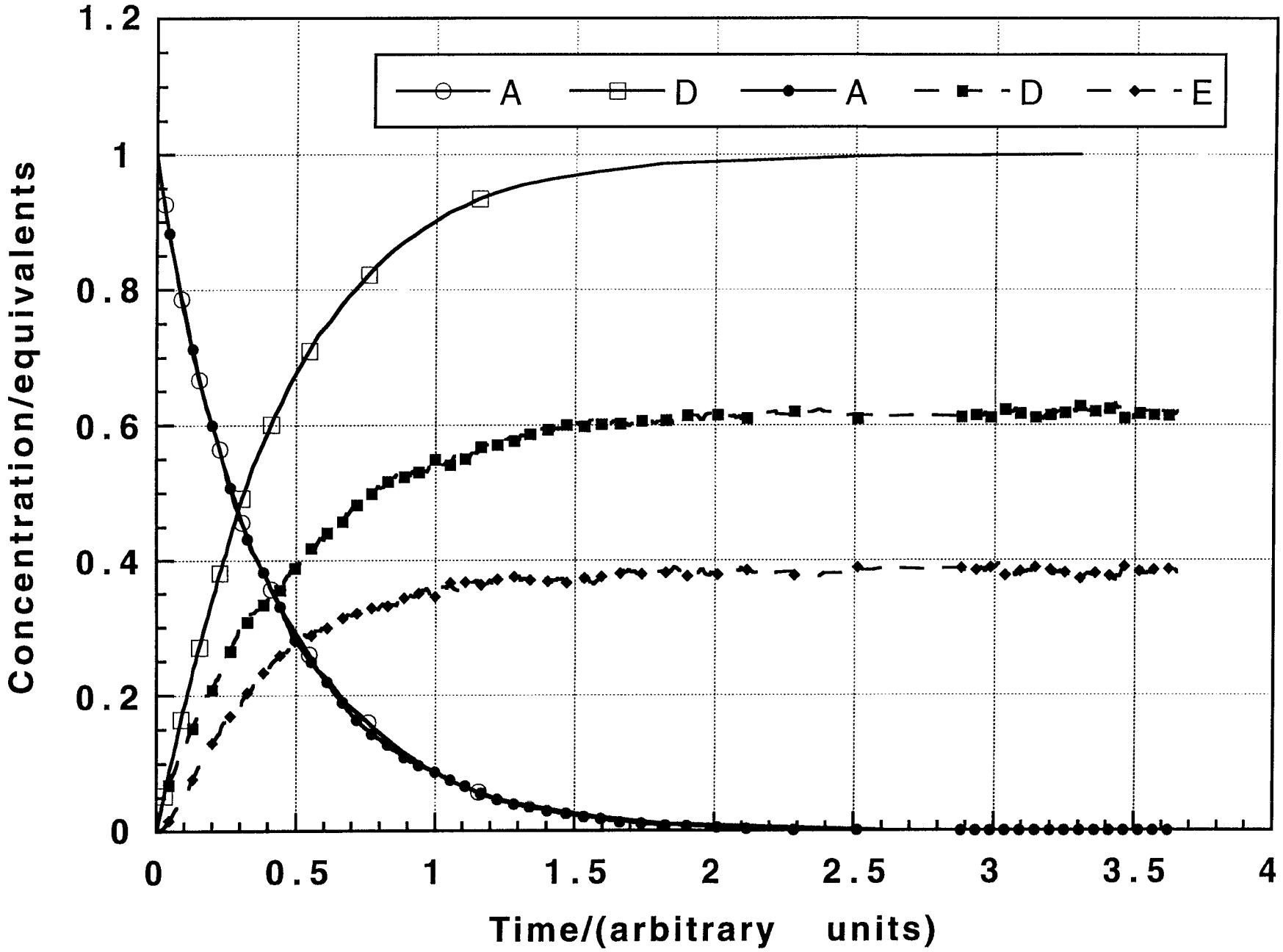

# Fig. 6. Synthetic Model Simulation (CKS): $[L_0] = 10$

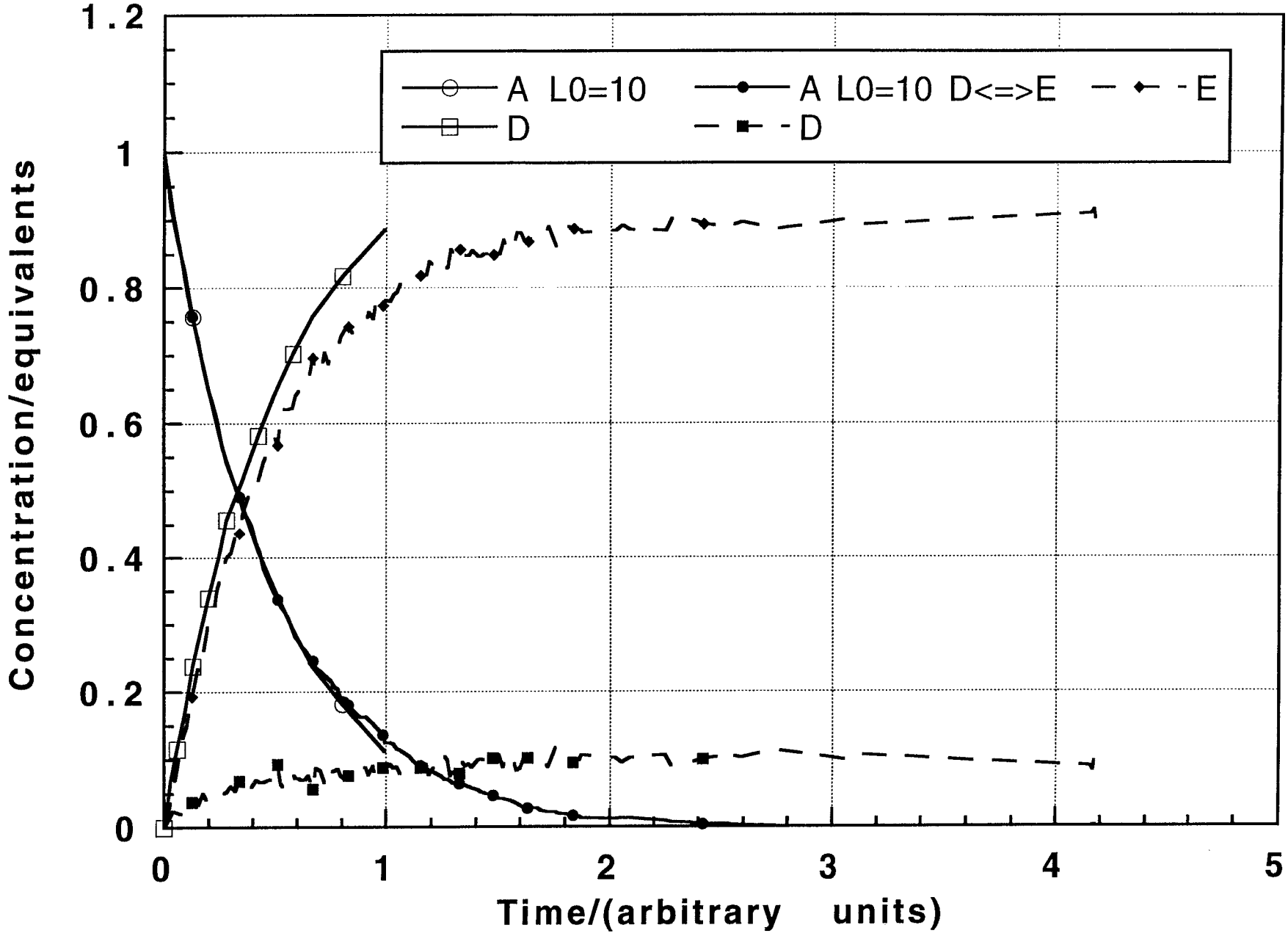

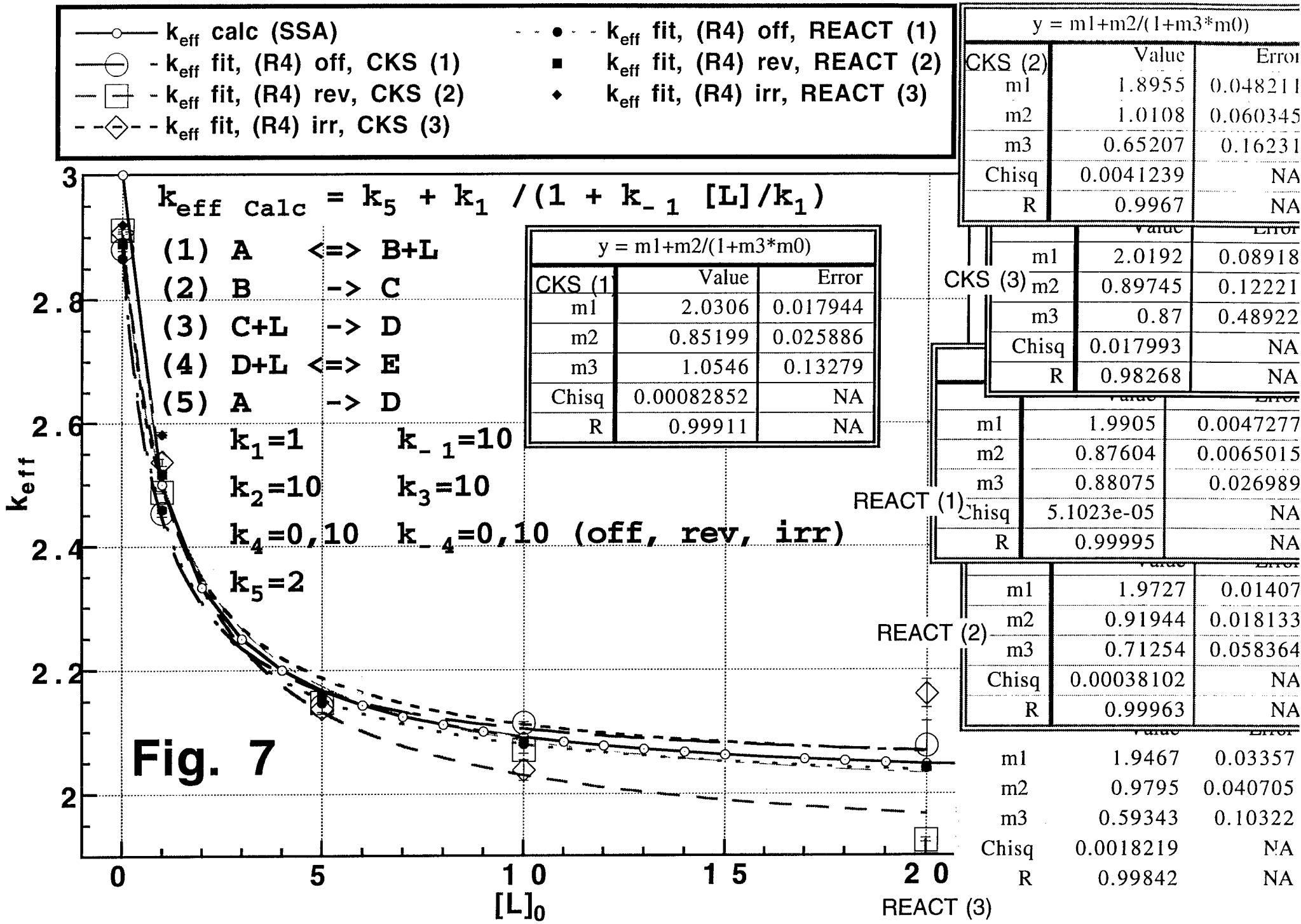


| y = m1+m2/(1+m3*m0) | | |
|---|---|---|
| CKS (1) | Value | Error |
| m1 | 2.0306 | 0.017944 |
| m2 | 0.85199 | 0.025886 |
| m3 | 1.0546 | 0.13279 |
| Chisq | 0.00082852 | NA |
| R | 0.99911 | NA |

| y = m1+m2/(1+m3*m0) | | |
|---|---|---|
| CKS (2) | Value | Error |
| m1 | 1.8955 | 0.048211 |
| m2 | 1.0108 | 0.060345 |
| m3 | 0.65207 | 0.16231 |
| Chisq | 0.0041239 | NA |
| R | 0.9967 | NA |

| CKS (3) | Value | Error |
|---|---|---|
| m1 | 2.0192 | 0.08918 |
| m2 | 0.89745 | 0.12221 |
| m3 | 0.87 | 0.48922 |
| Chisq | 0.017993 | NA |
| R | 0.98268 | NA |

| REACT (1) | Value | Error |
|---|---|---|
| m1 | 1.9905 | 0.0047277 |
| m2 | 0.87604 | 0.0065015 |
| m3 | 0.88075 | 0.026989 |
| Chisq | 5.1023e-05 | NA |
| R | 0.99995 | NA |

| REACT (2) | Value | Error |
|---|---|---|
| m1 | 1.9727 | 0.01407 |
| m2 | 0.91944 | 0.018133 |
| m3 | 0.71254 | 0.058364 |
| Chisq | 0.00038102 | NA |
| R | 0.99963 | NA |

| REACT (3) | Value | Error |
|---|---|---|
| m1 | 1.9467 | 0.03357 |
| m2 | 0.9795 | 0.040705 |
| m3 | 0.59343 | 0.10322 |
| Chisq | 0.0018219 | NA |
| R | 0.99842 | NA |

**Fig. 8. Free ligand dependence of the isomerization of compound(1) $Ru(PMe_3)_3\{\eta^4\text{-endo-o-}C_6Me_4(CH_2)_2\}$**

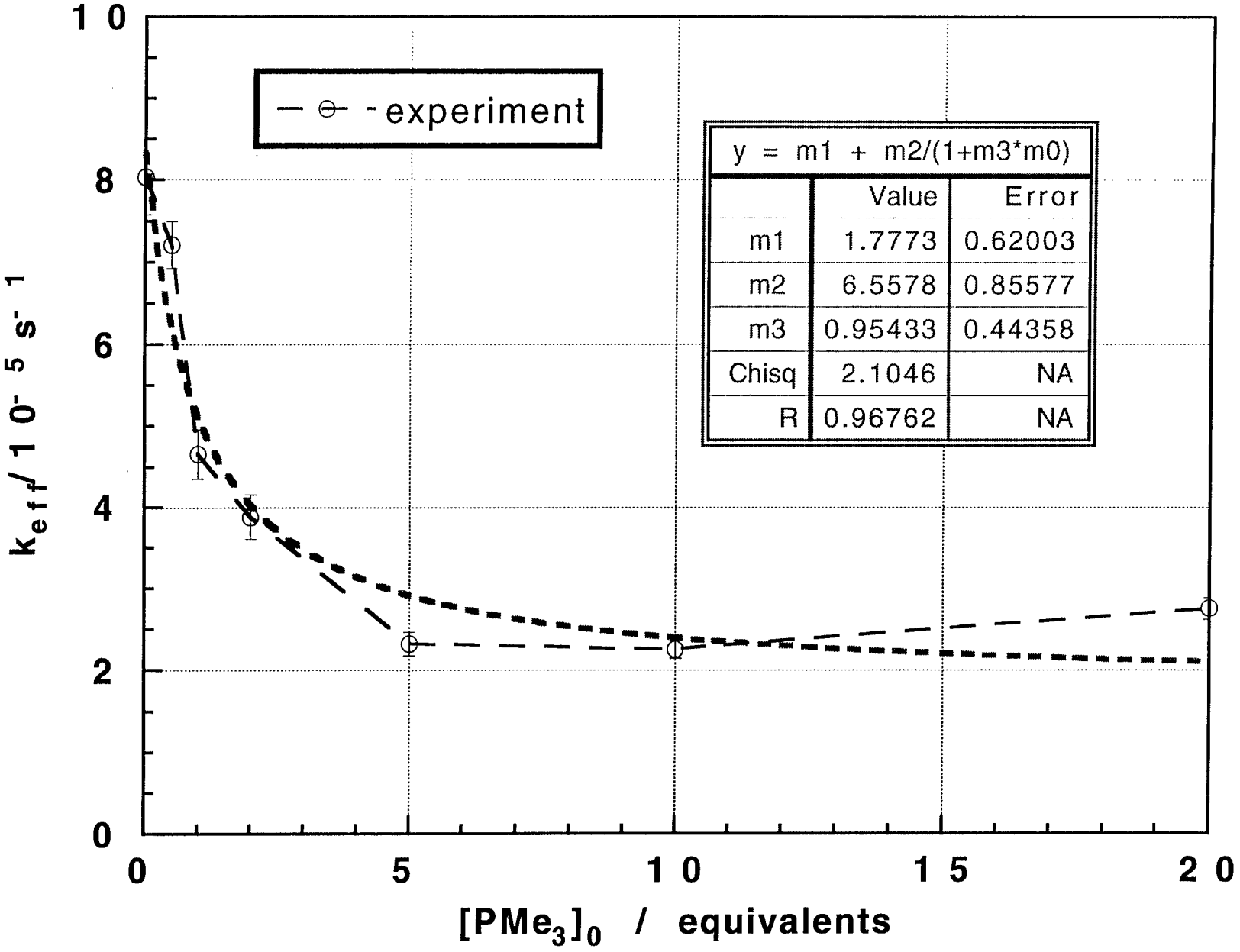

**Fig. 9. Simulation (CKS) of the isomerization of compound(1) $Ru(PMe_3)_3\{\eta^4\text{-endo-o-}C_6Me_4(CH_2)_2\}$ [L0]=0**

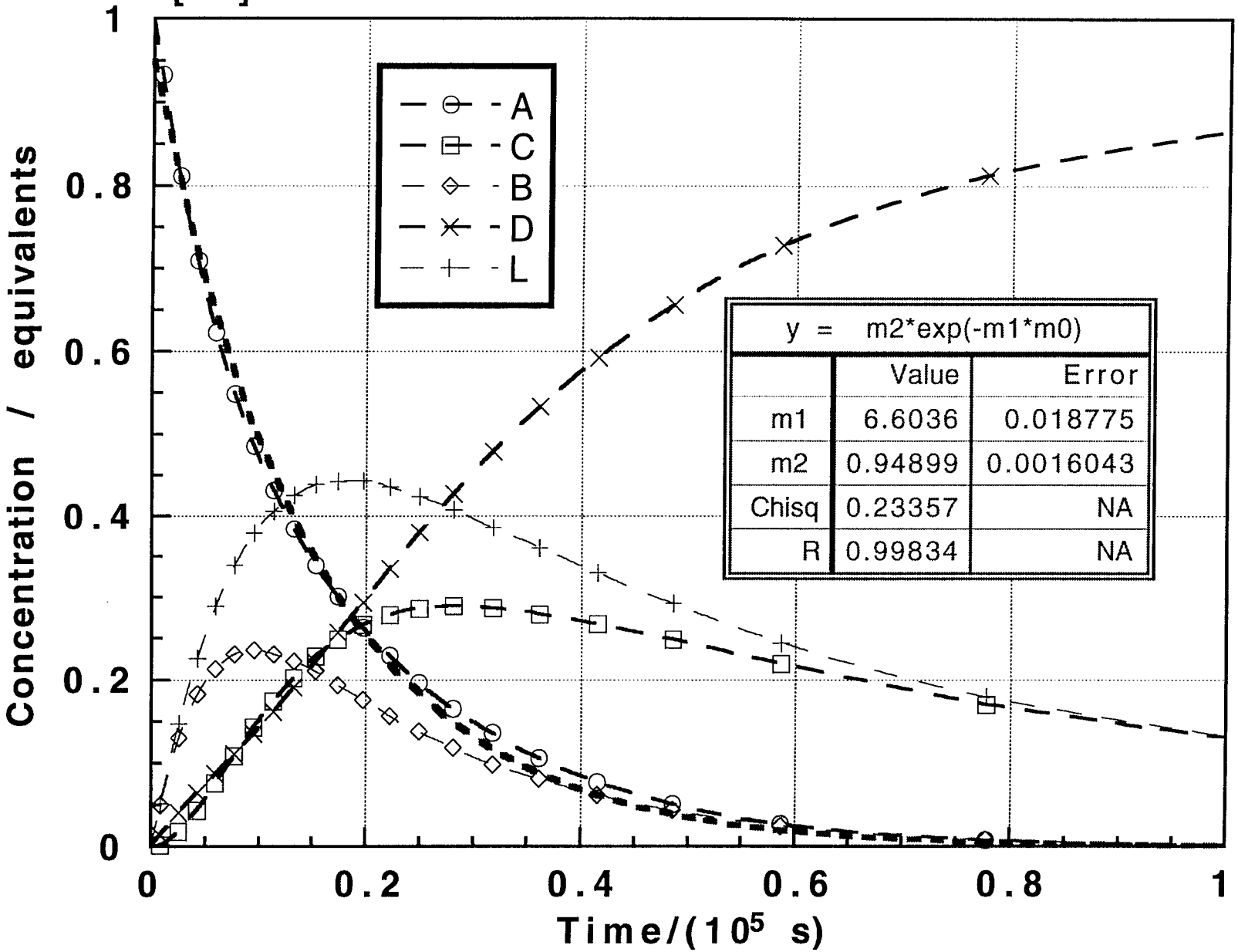

**Fig. 10. Simulation (CKS) of the isomerization of compound(1) $Ru(PMe_3)_3\{\eta^4\text{-endo-o-}C_6Me_4(CH_2)_2\}$**

$[L_0]=1$

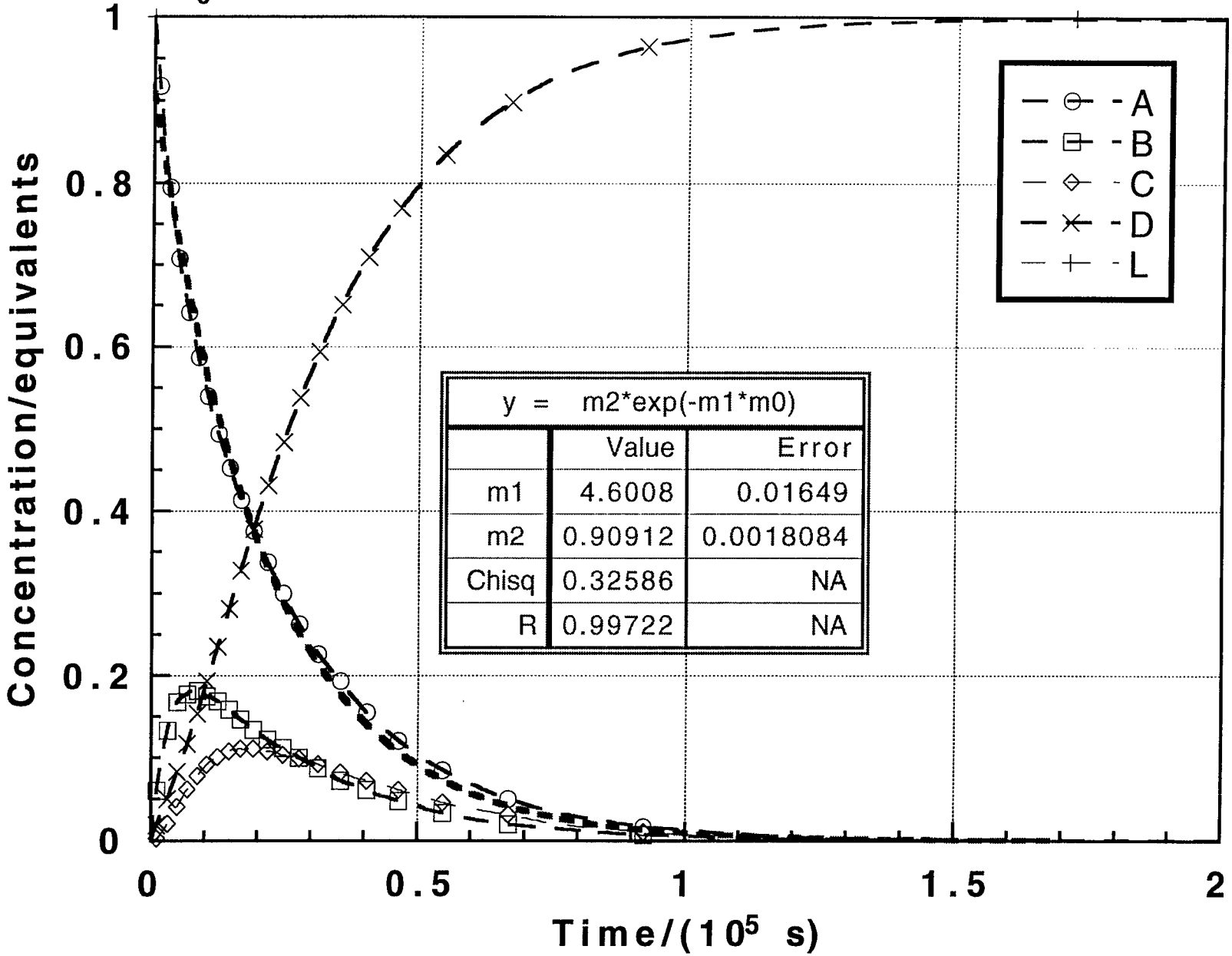


| y = m2*exp(-m1*m0) | | |
|---|---|---|
| | Value | Error |
| m1 | 4.6008 | 0.01649 |
| m2 | 0.90912 | 0.0018084 |
| Chisq | 0.32586 | NA |
| R | 0.99722 | NA |

**Fig. 11. Simulation (CKS) of the isomerization of compound(1) $Ru(PMe_3)_3\{\eta^4\text{-endo-o-}C_6Me_4(CH_2)_2\}$ $[L_0]=10$**

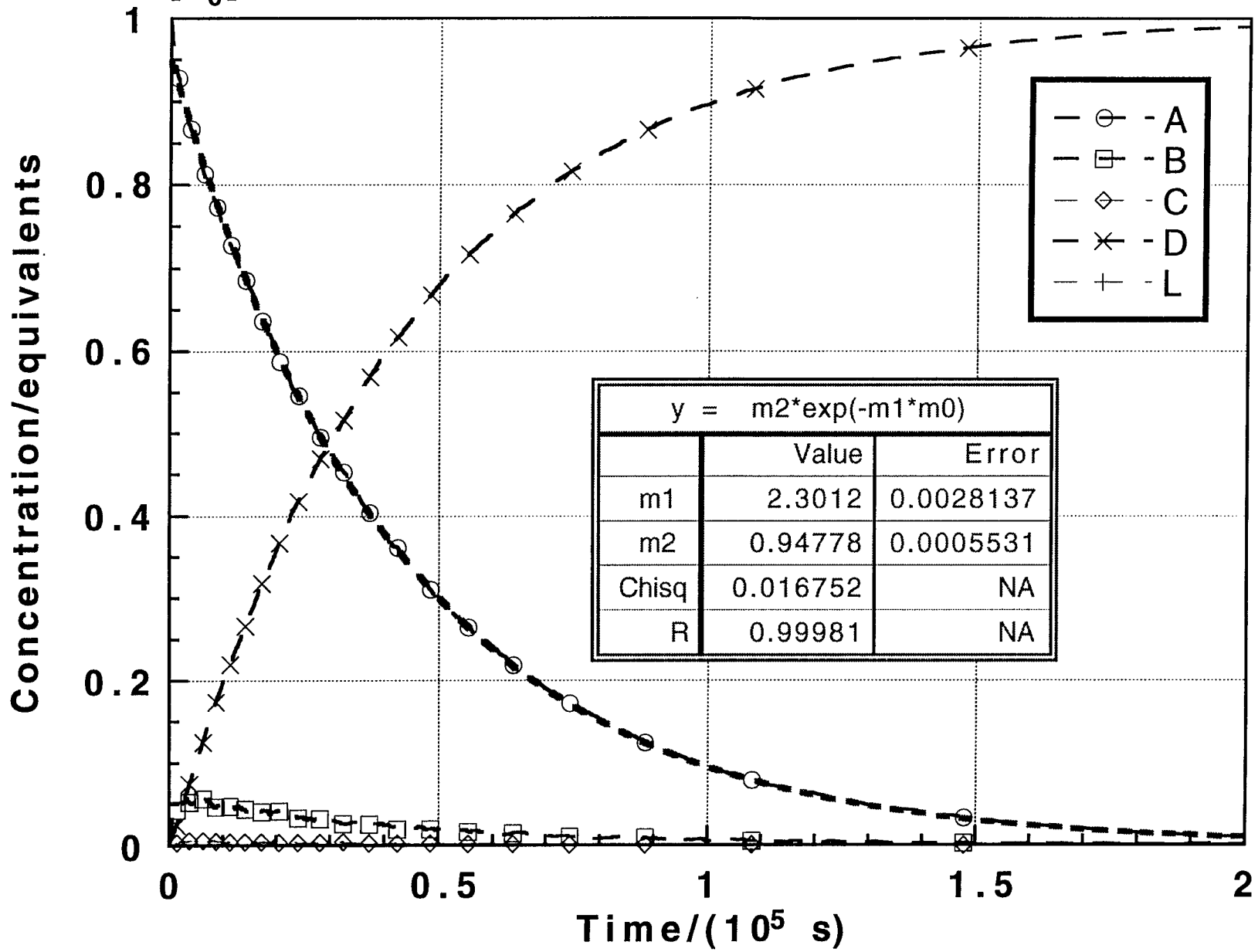


| y = m2*exp(-m1*m0) | | |
|---|---|---|
| | Value | Error |
| m1 | 2.3012 | 0.0028137 |
| m2 | 0.94778 | 0.0005531 |
| Chisq | 0.016752 | NA |
| R | 0.99981 | NA |

Fig. 12. Free ligand dependence of the isomerization of compound(1) $Ru(PMe_3)_3\{\eta^4\text{-endo-o-}C_6Me_4(CH_2)_2\}$

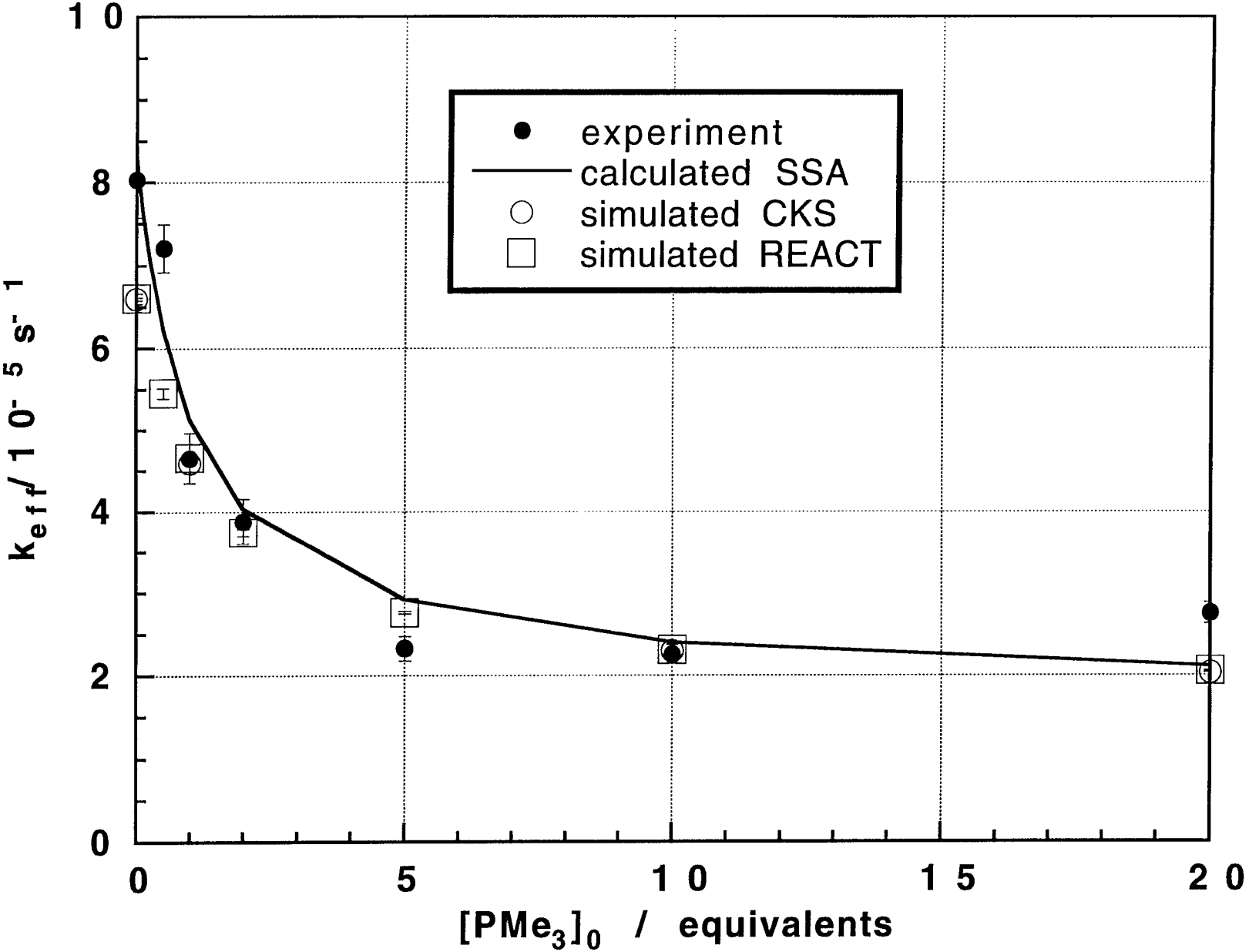

**Fig. 13. Free ligand dependence of the isomerization of compound(3) $Os(PMe_2Ph)_3\{\eta^4\text{-endo-o-}C_6Me_4(CH_2)_2\}$**

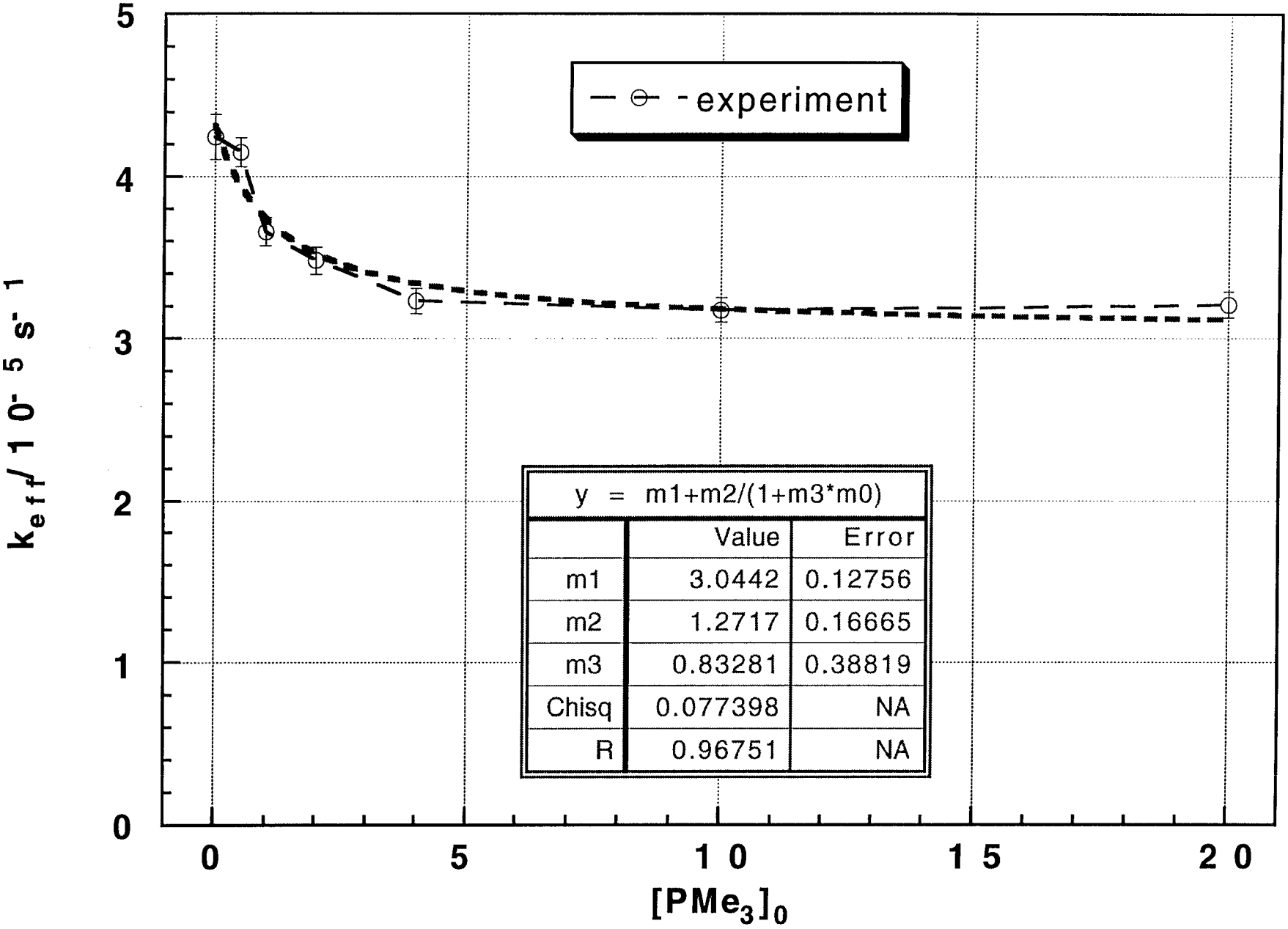


| y = m1+m2/(1+m3*m0) | | |
|---|---|---|
| | Value | Error |
| m1 | 3.0442 | 0.12756 |
| m2 | 1.2717 | 0.16665 |
| m3 | 0.83281 | 0.38819 |
| Chisq | 0.077398 | NA |
| R | 0.96751 | NA |

**Fig. 14. Free ligand dependence of the isomerization of compound(2) $Os(PMe_3)_3\{\eta^4\text{-endo-o-}C_6Me_4(CH_2)_2\}$**

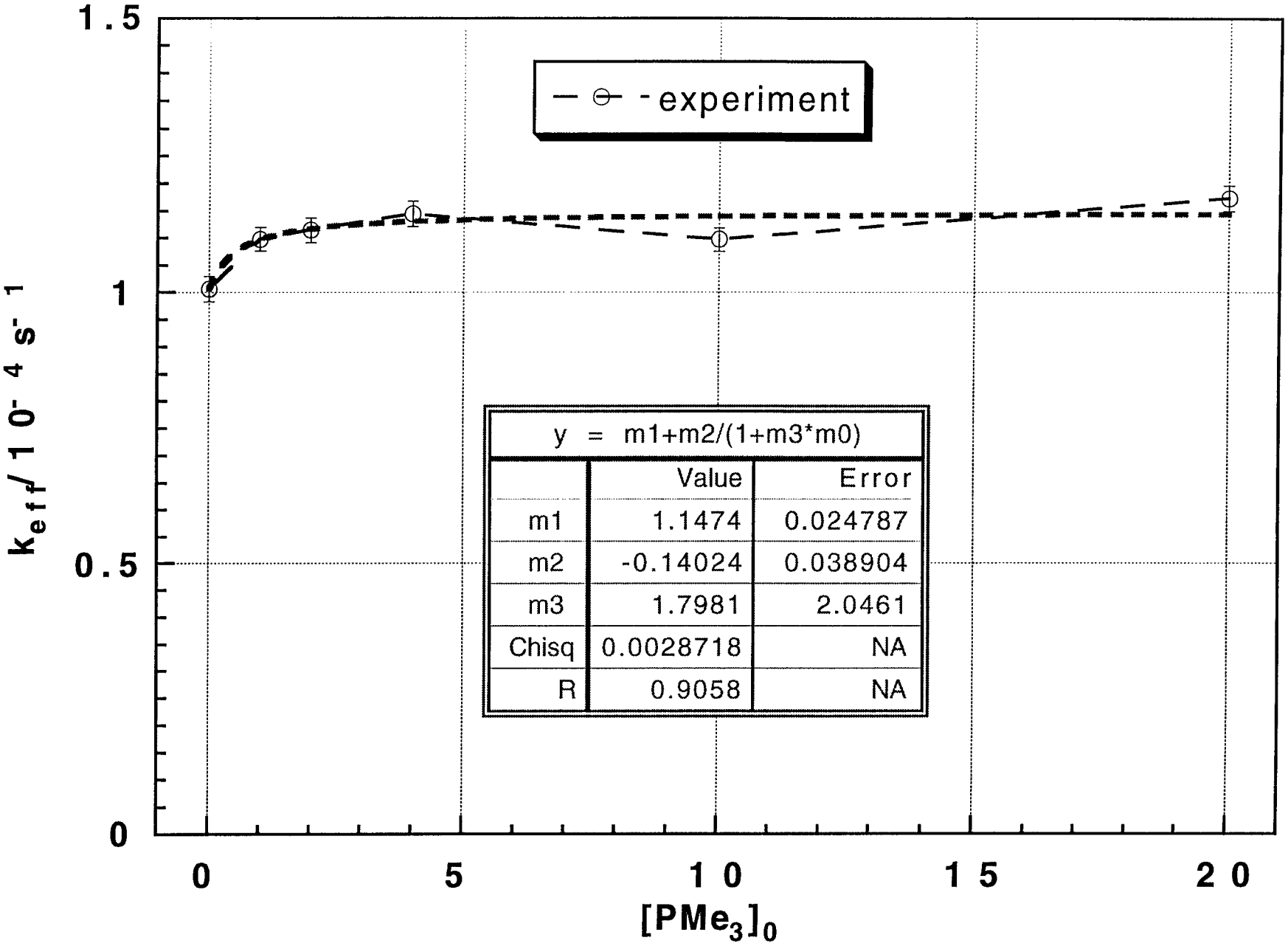


| y = m1+m2/(1+m3*m0) | | |
|---|---|---|
| | Value | Error |
| m1 | 1.1474 | 0.024787 |
| m2 | -0.14024 | 0.038904 |
| m3 | 1.7981 | 2.0461 |
| Chisq | 0.0028718 | NA |
| R | 0.9058 | NA |

**Fig. 15. Free ligand dependence of the isomerization of compound(2) $Os(PMe_3)_3\{\eta^4\text{-endo-o-}C_6Me_4(CH_2)_2\}$**

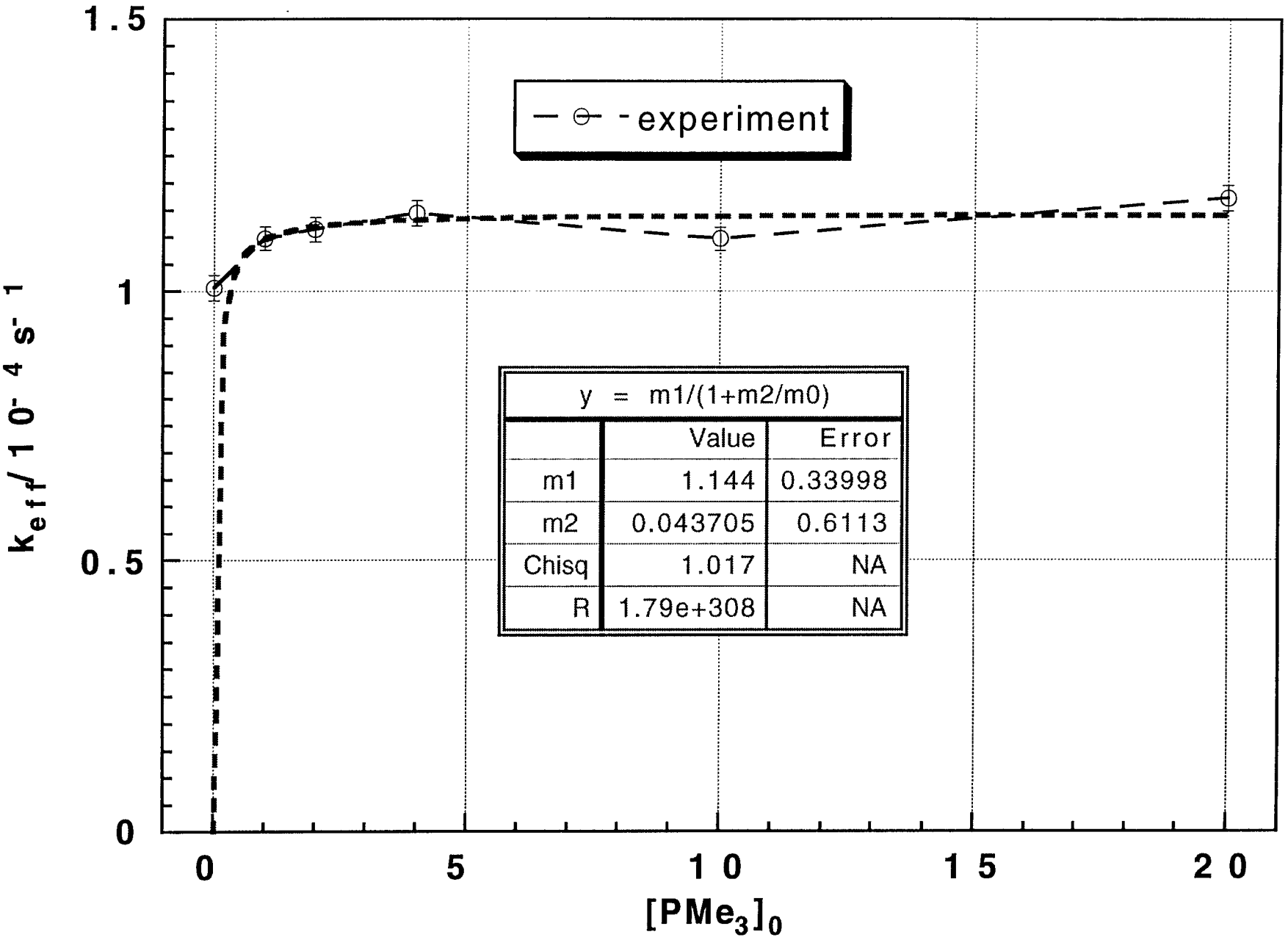

**Fig. 16. Simulation of the isomerization of compound(2) $Os(PMe_3)_3\{\eta^4\text{-endo-o-}C_6Me_4(CH_2)_2\}$**

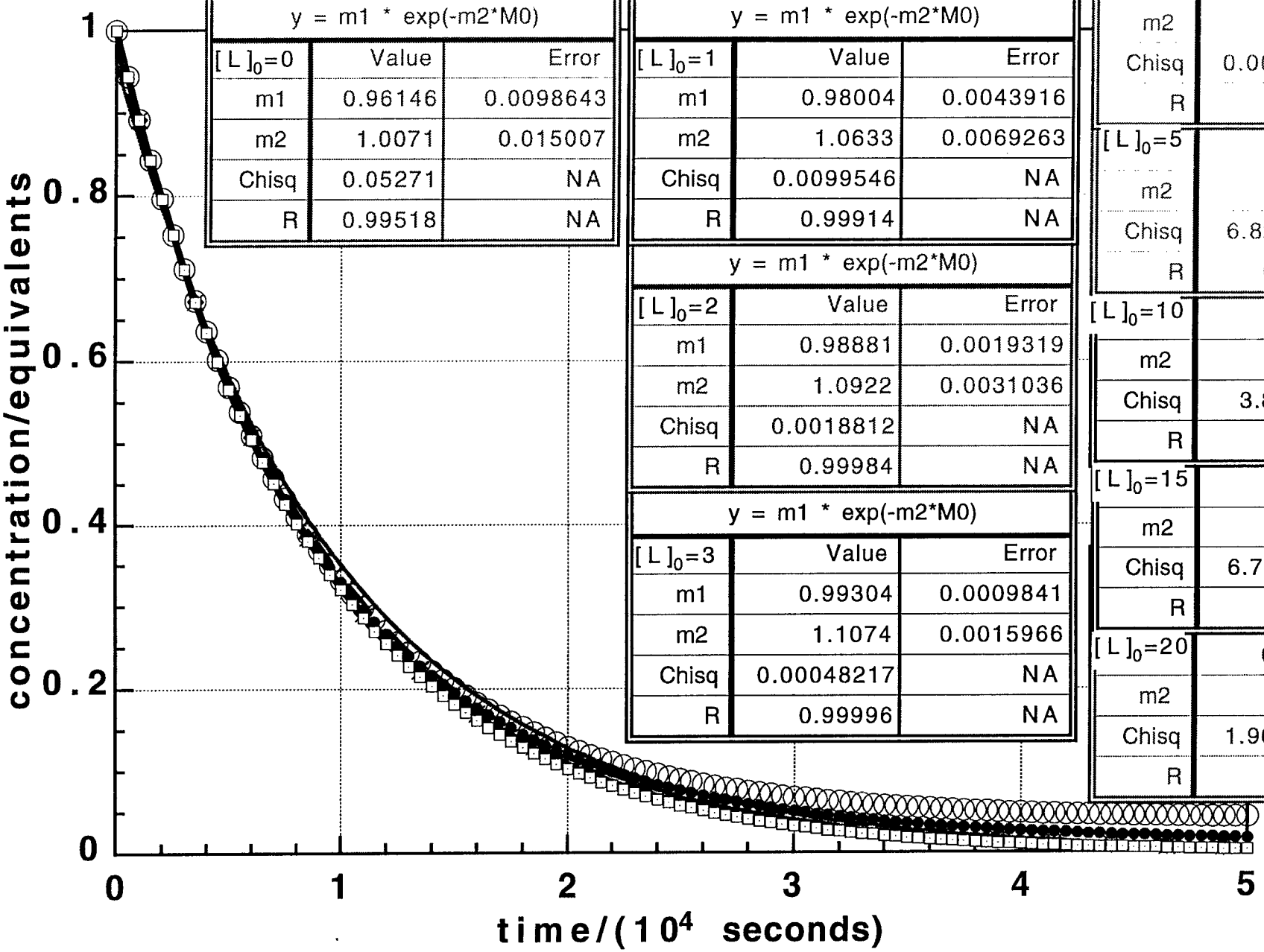


| y = m1 * exp(-m2*M0) | | |
|---|---|---|
| $[L]_0$=0 | Value | Error |
| m1 | 0.96146 | 0.0098643 |
| m2 | 1.0071 | 0.015007 |
| Chisq | 0.05271 | NA |
| R | 0.99518 | NA |

| y = m1 * exp(-m2*M0) | | |
|---|---|---|
| $[L]_0$=1 | Value | Error |
| m1 | 0.98004 | 0.0043916 |
| m2 | 1.0633 | 0.0069263 |
| Chisq | 0.0099546 | NA |
| R | 0.99914 | NA |

| y = m1 * exp(-m2*M0) | | |
|---|---|---|
| $[L]_0$=2 | Value | Error |
| m1 | 0.98881 | 0.0019319 |
| m2 | 1.0922 | 0.0031036 |
| Chisq | 0.0018812 | NA |
| R | 0.99984 | NA |

| y = m1 * exp(-m2*M0) | | |
|---|---|---|
| $[L]_0$=3 | Value | Error |
| m1 | 0.99304 | 0.0009841 |
| m2 | 1.1074 | 0.0015966 |
| Chisq | 0.00048217 | NA |
| R | 0.99996 | NA |

| y = m1 * exp(-m2*M0) | | |
|---|---|---|
| $[L]_0$=4 | Value | Error |
| m1 | 0.99528 | 0.0005761 |
| m2 | 1.1162 | 0.0009402 |
| Chisq | 0.00016412 | NA |
| R | 0.99999 | NA |
| $[L]_0$=5 | 0.9966 | 0.0003722 |
| m2 | 1.1218 | 0.0006097 |
| Chisq | 6.8207e-05 | NA |
| R | 0.99999 | NA |
| $[L]_0$=10 | 0.9989 | 8.8808e-05 |
| m2 | 1.1333 | 0.00014667 |
| Chisq | 3.847e-06 | NA |
| R | 1 | NA |
| $[L]_0$=15 | 0.99946 | 3.7329e-05 |
| m2 | 1.1371 | 6.1823e-05 |
| Chisq | 6.7768e-07 | NA |
| R | 1 | NA |
| $[L]_0$=20 | 0.99968 | 2.0128e-05 |
| m2 | 1.1389 | 3.3383e-05 |
| Chisq | 1.9675e-07 | NA |
| R | 1 | NA |

Fig. 17. Simulation of the isomerization of compound(2) $Os(PMe_3)_3\{\eta^4\text{-endo-o-}C_6Me_4(CH_2)_2\}$

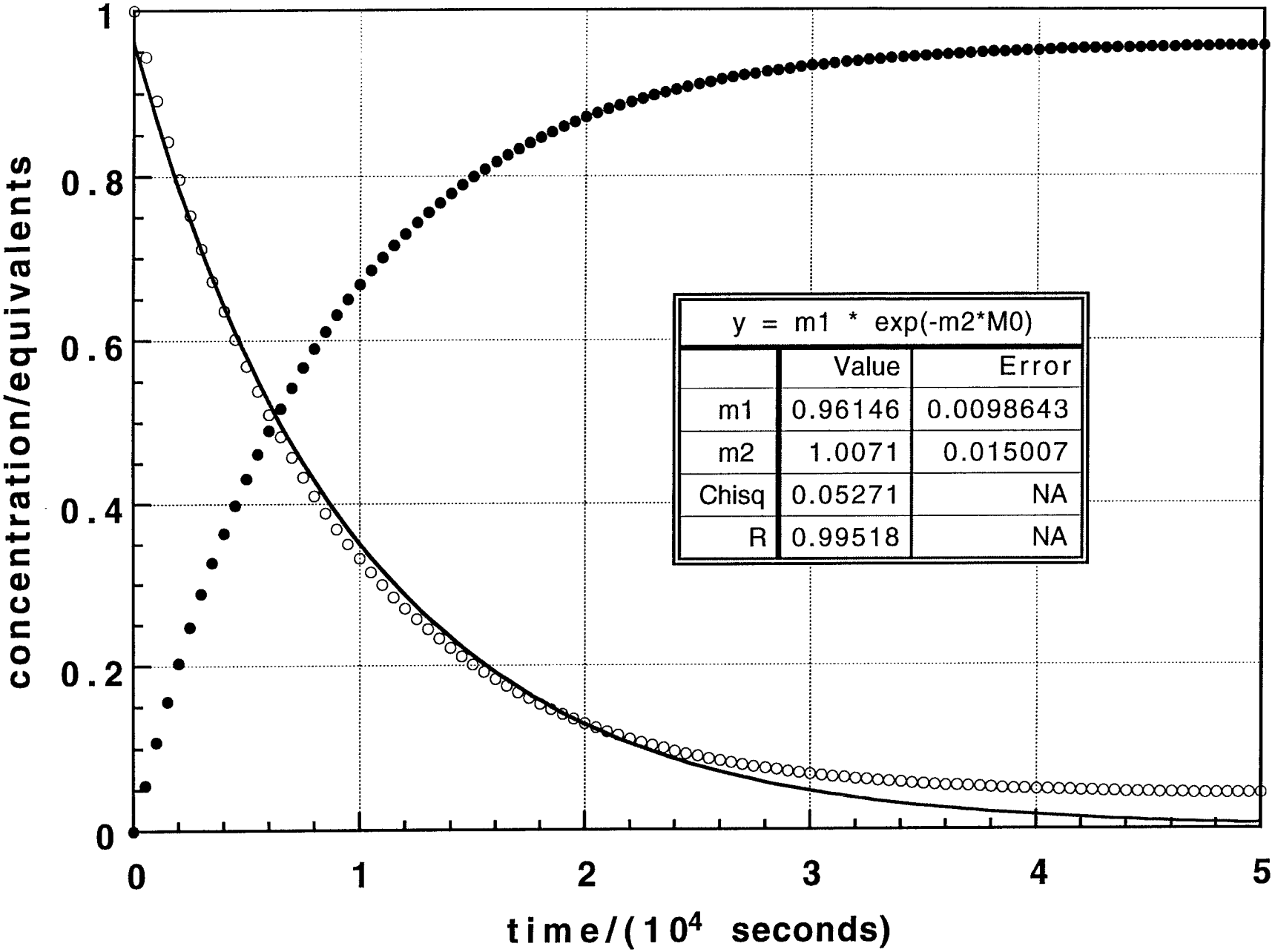

**Fig. 18. Simulation of the isomerization of compound(2) $Os(PMe_3)_3\{\eta^4\text{-endo-o-}C_6Me_4(CH_2)_2\}$**

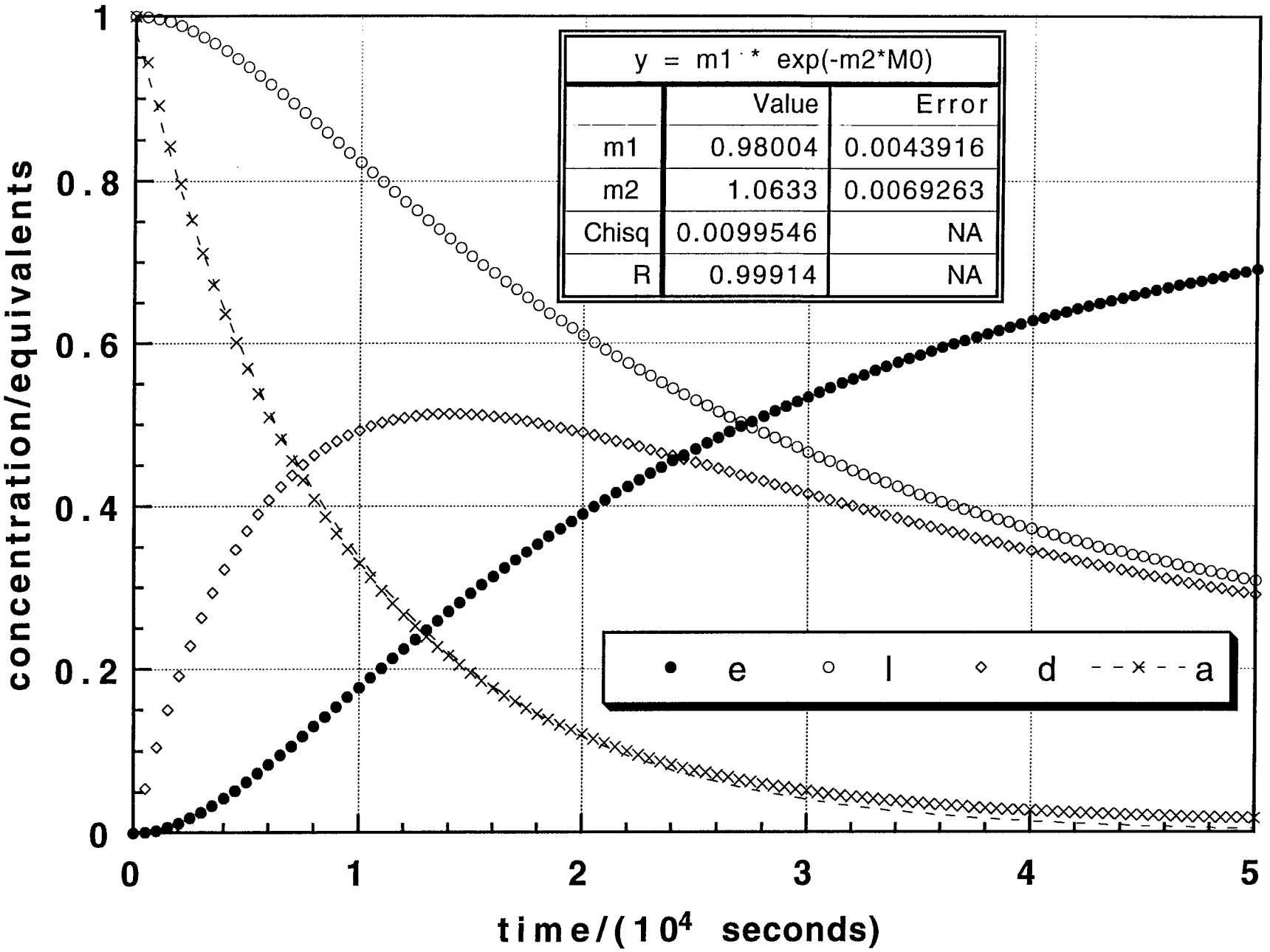

**Fig. 19. Simulation of the isomerization of compound(2) $Os(PMe_3)_3\{\eta^4\text{-endo-o-}C_6Me_4(CH_2)_2\}$**

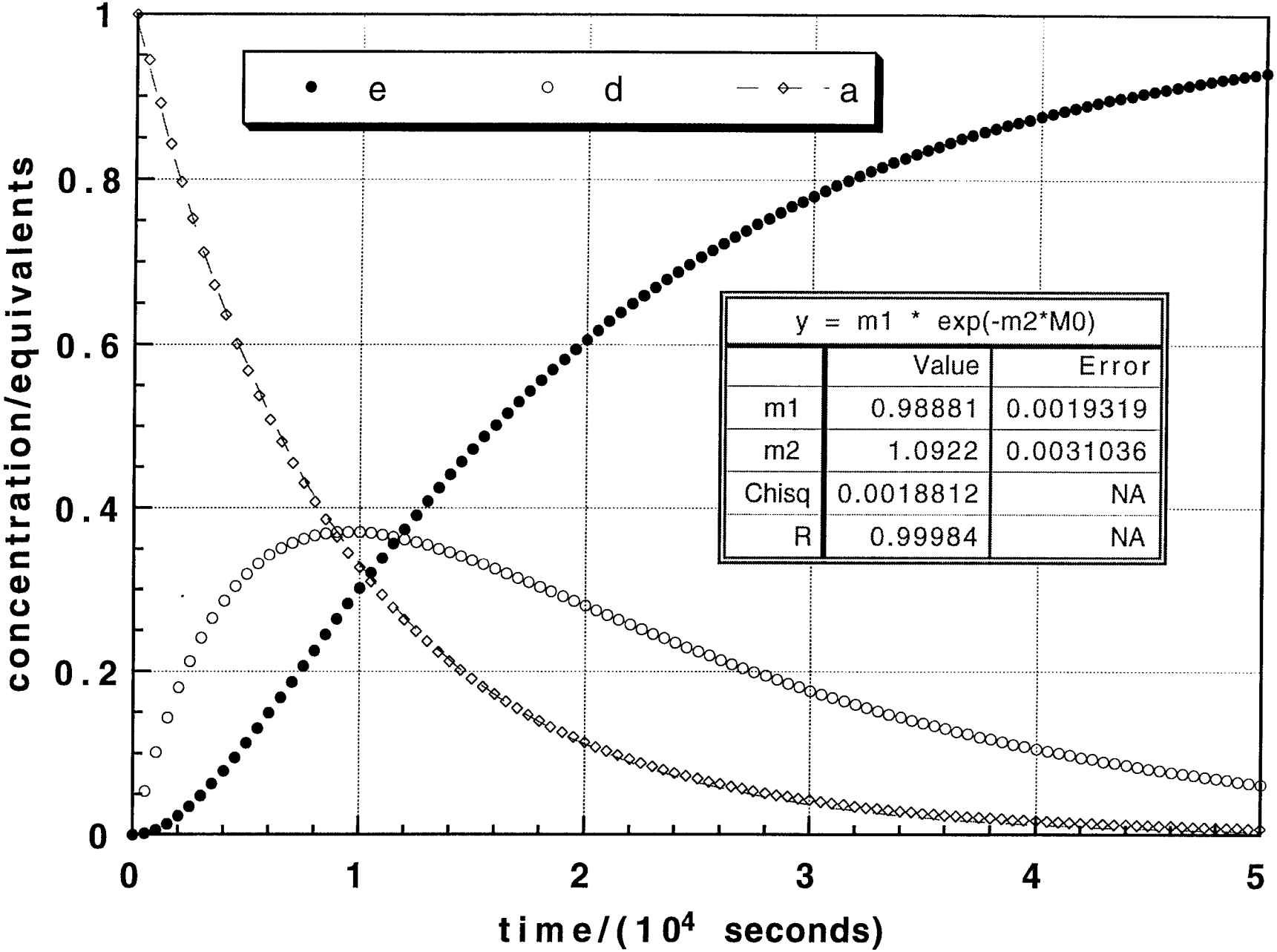

Fig. 20. Simulation of the isomerization of compound(2) $Os(PMe_3)_3\{\eta^4\text{-endo-o-}C_6Me_4(CH_2)_2\}$

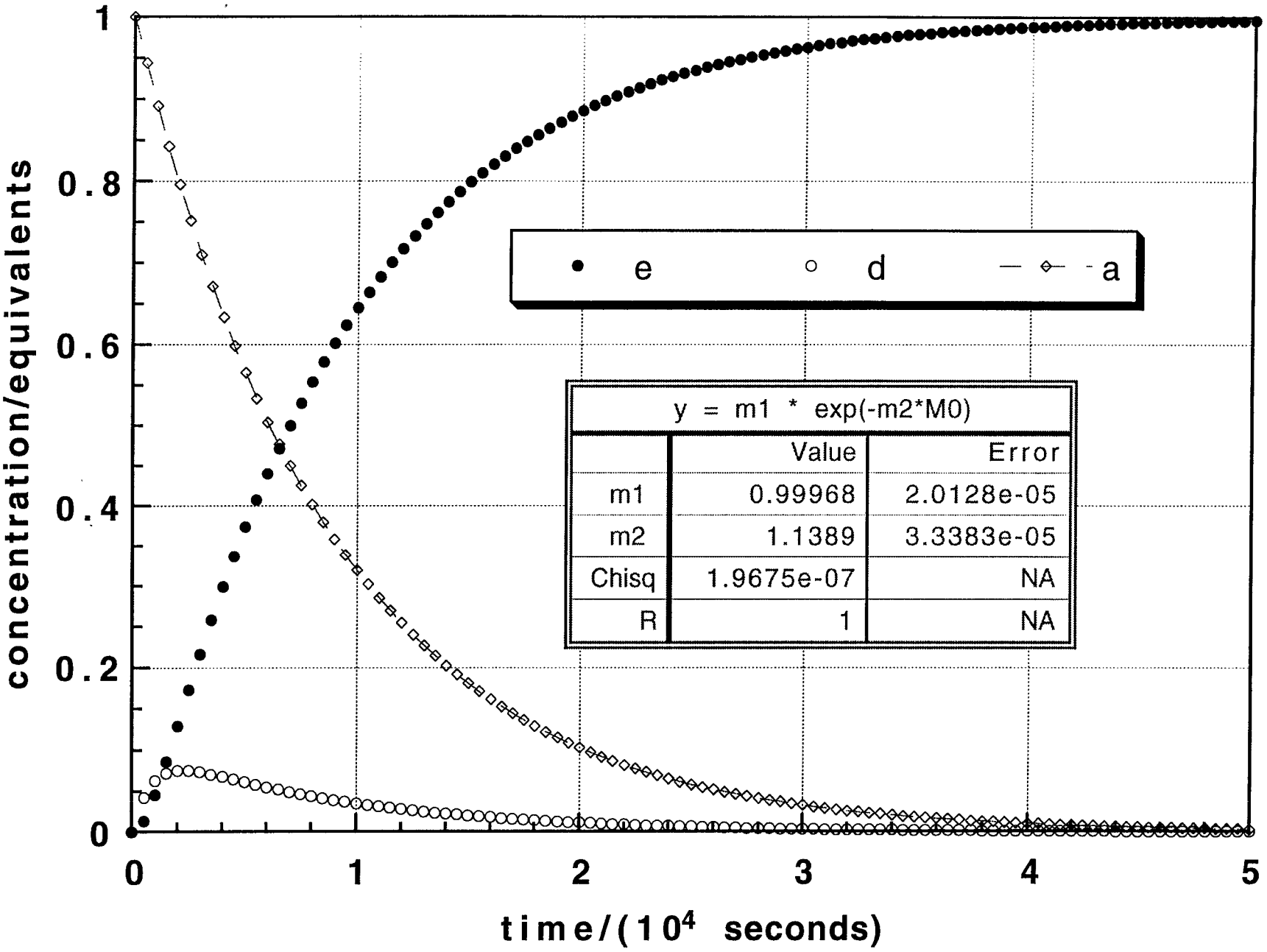

**Fig. 21. Experiment and Simulation of the isomerization of compound(2) $Os(PMe_3)_3\{\eta^4\text{-endo-o-}C_6Me_4(CH_2)_2\}$**

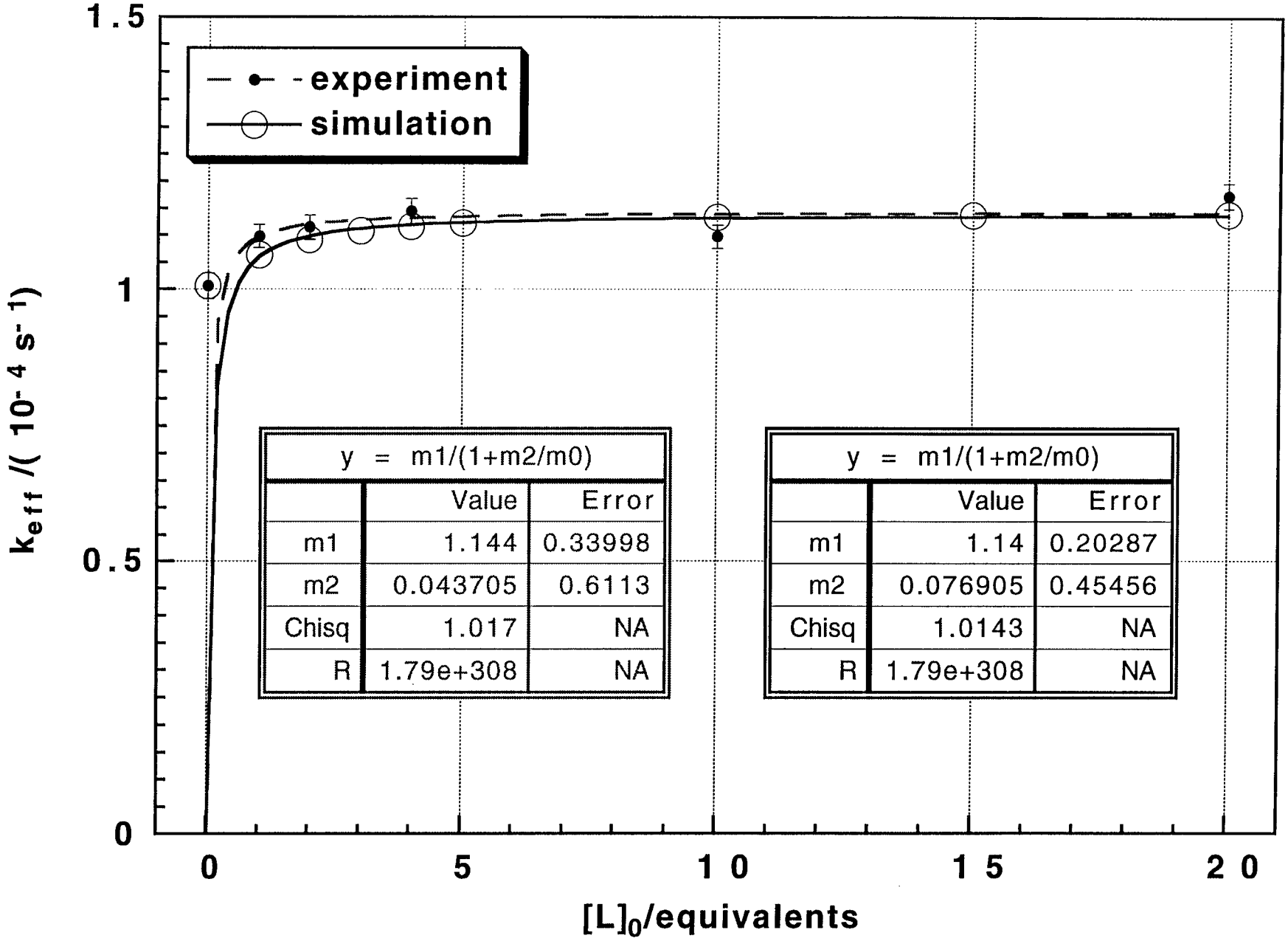


| y = m1/(1+m2/m0) | | |
|---|---|---|
| | Value | Error |
| m1 | 1.144 | 0.33998 |
| m2 | 0.043705 | 0.6113 |
| Chisq | 1.017 | NA |
| R | 1.79e+308 | NA |

| y = m1/(1+m2/m0) | | |
|---|---|---|
| | Value | Error |
| m1 | 1.14 | 0.20287 |
| m2 | 0.076905 | 0.45456 |
| Chisq | 1.0143 | NA |
| R | 1.79e+308 | NA |

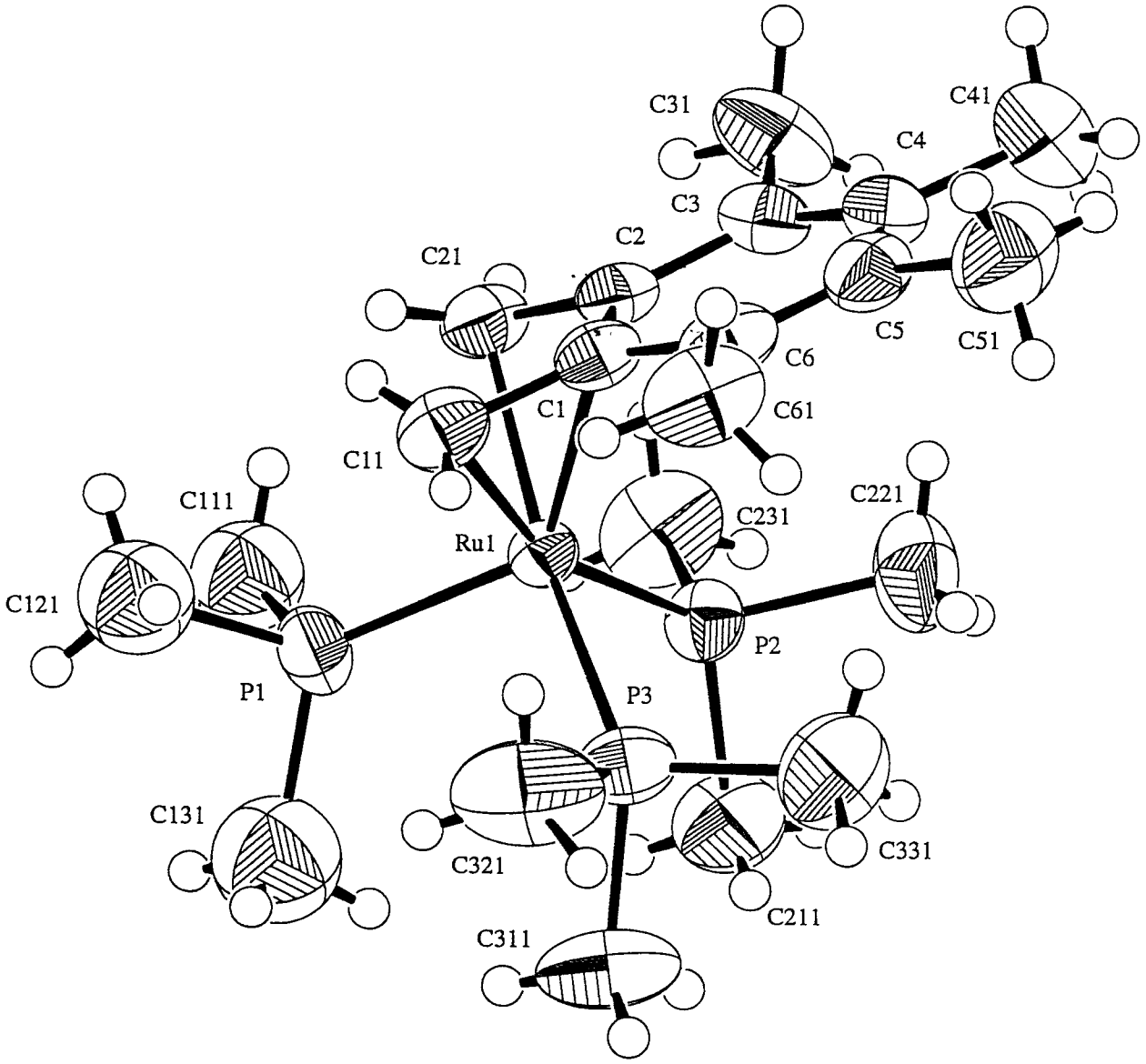
C31
C41
C4
C3
C2
C21
C5
C51
C6
C1
C61
C11
C111
C221
C231
Ru1
C121
P2
P1
P3
C131
C321
C331
C211
C311

*Experimental*

Data Collection

A yellow plate like crystal of $C_{21}H_{43}P_3Ru$ having approximate dimensions of 0.88 x 0.18 x 0.32 mm was mounted in a 0.7 mm glass capillary under argon. All measurements were made on a Rigaku AFC6S diffractometer with graphite monochromated Mo-K$\alpha$ radiation.

Cell constants and an orientation matrix for data collection, obtained from a least-squares refinement using the setting angles of 25 carefully centered reflections in the range $34.85 < 2\theta < 43.04^o$ corresponded to a primitive orthorhombic cell with dimensions:

a = 16.638(4) Å
b = 18.233(6) Å
c = 16.635(4) Å
V = 5046(2) Å$^3$

For Z = 8 and F.W. = 489.56, the calculated density is 1.29 g/cm$^3$. The systematic absences of:

0kl: $k \pm 2n$
h0l: $l \pm 2n$
hk0: $h \pm 2n$

uniquely determine the space group to be:

Pbca (#61)

The data were collected at a temperature of 23 $\pm$ 1°C using the $\omega$-2$\theta$ scan technique to a maximum 2$\theta$ value of 50.1°.Omega scans of several intense reflections, made prior to data collection, had an average width at half-height of 0.34° with a take-off angle of 6.0°. Scans of (1.20 + 0.34 tan $\theta$)° were made at a speed of 2.0°/min (in $\omega$). The weak reflections ($I < 10.0\sigma(I)$) were rescanned (maximum of 4 scans) and the counts were accumulated to ensure good counting statistics. Stationary background counts were recorded on each side of the reflection. The ratio of peak counting time to background counting time was 2:1. The diameter of the incident beam collimator was 1.0 mm, the crystal to detector distance was 400 mm, and the detector aperture was 9.0 x 13.0 mm (horizontal x vertical).

Data Reduction

A total of 4980 reflections was collected. The intensities of three representative reflection were measured after every 150 reflections. No decay correction was applied.

The linear absorption coefficient, $\mu$, for Mo-k$\alpha$ radiation is 8.0 cm$^{-1}$. An empirical absorption correction based on azimuthal scans of several reflections was applied which resulted in transmission factors ranging from 0.79 to 1.00. The data were corrected for Lorentz and polarization effects. A correction for secondary extinction was applied (coefficient = 4.38672e-08).

Structure Solution and Refinement

The structure was solved by heavy-atom Patterson methods[1] and expanded using Fourier techniques[2]. Some non-hydrogen atoms were refined anisotropically, while the rest were refined isotropically. Hydrogen atoms were included but not refined. The final cycle of full-matrix least-squares refinement[3] was based on 3238 observed reflections ($I > 3.00\sigma(I)$) and 224 variable parameters and converged (largest parameter shift was 0.02 times its esd) with unweighted and weighted agreement factors of:

$$R = \Sigma \, ||Fo| - |Fc|| \, / \, \Sigma \, |Fo| = 0.032$$

$$R_w = [( \Sigma \, w \, (|Fo| - |Fc|)^2 \, / \, \Sigma \, w \, Fo^2)]^{1/2} = 0.037$$

The standard deviation of an observation of unit weight[4] was 2.05. The weighting scheme was based on counting statistics and included a factor ($p = 0.020$) to downweight the intense reflections. Plots of $\Sigma \, w \, (|Fo| - |Fc|)^2$ versus |Fo|,reflection order in data collection, $\sin \theta/\lambda$ and various classes of indices showed no unusual trends. The maximum and minimum peaks on the final difference Fourier map corresponded to 0.61 and -0.34 $e^-/Å^3$, respectively.

Neutral atom scattering factors were taken from Cromer and Waber[5]. Anomalous dispersion effects were included in Fcalc[6]; the values for $\Delta f'$ and $\Delta f''$ were those of Creagh and McAuley[7]. The values for the mass attenuation coefficients are those of Creagh and Hubbel[8]. All calculations were performed using the teXsan[9] crystallographic software package of Molecular Structure Corporation.

*References*

(1) PATTY: Beurskens, P.T., Admiraal, G., Beurskens, G., Bosman, W.P., Garcia-Granda, S., Gould, R.O., Smits, J.M.M. and Smykalla, C. (1992). The DIRDIF program system, Technical Report of the Crystallography Laboratory, University of Nijmegen, The Netherlands.

(2) DIRDIF94: Beurskens, P.T., Admiraal, G., Beurskens, G., Bosman, W.P., de Gelder, R., Israel, R. and Smits, J.M.M.(1994). The DIRDIF-94 program system, Technical Report of the Crystallography Laboratory, University of Nijmegen, The Netherlands.

(3) Least-Squares:

Function minimized: $\Sigma\omega(|F_o|-|F_c|)^2$

where $\omega = 4F_o^2/\sigma^2(F_o^2) = [\sigma^2(F_o) + (pF_o/2)^2]^{-1}$

$F_o^2 = \Sigma(C-RB)/Lp$

and $\sigma^2(F_o^2) = [S^2(C+R^2B) + (pF_o^2)^2]/Lp^2$

S = Scan rate
C = Total integrated peak count
R = Ratio of scan time to background counting time

B = Total background count
Lp = Lorentz-polarization factor
$p$ = p-factor

(4) Standard deviation of an observation of unit weight:

$$[\Sigma w(|F_o|-|F_c|)^2/(N_o-N_v)]^{1/2}$$

where: $N_o$ = number of observations

$N_v$ = number of variables

(5) Cromer, D. T. & Waber, J. T.; "International Tables for X-ray Crystallography", Vol. IV, The Kynoch Press, Birmingham, England, Table 2.2 A (1974).

(6) Ibers, J. A. & Hamilton, W. C.; Acta Crystallogr., 17, 781 (1964).

(7) Creagh, D. C. & McAuley, W.J .; "International Tables for Crystallography", Vol C, (A.J.C. Wilson, ed.), Kluwer Academic Publishers, Boston; Table 4.2.6.8, pages 219-222 (1992).

(8) Creagh, D. C. & Hubbell, J.H..; "International Tables for Crystallography", Vol C, (A.J.C. Wilson, ed.), Kluwer Academic Publishers, Boston, Table 4.2.4.3, pages 200-206 (1992).

(9) teXsan: Crystal Structure Analysis Package, Molecular Structure Corporation (1985 & 1992).

*EXPERIMENTAL DETAILS*

A. Crystal Data

| | |
|---|---|
| Empirical Formula | $C_{21}H_{43}P_3Ru$ |
| Formula Weight | 489.56 |
| Crystal Color, Habit | yellow, plate |
| Crystal Dimensions | 0.88 X 0.18 X 0.32 mm |
| Crystal System | orthorhombic |
| Lattice Type | Primitive |
| No. of Reflections Used for Unit Cell Determination (2θ range) | 25 ( 34.8 - 43.0° ) |
| Max/min hkl | 0, 19<br>0, 21<br>0, 19 |
| Omega Scan Peak Width at Half-height | 0.34° |
| Lattice Parameters | a = 16.638(4)Å<br>b = 18.233(6) Å<br>c = 16.635(4) Å<br>V = 5046(2) Å$^3$ |
| Space Group | Pbca (#61) |
| Z value | 8 |
| $D_{calc}$ | 1.289 g/cm$^3$ |
| $F_{000}$ | 2064.00 |
| MU(MoKALPHA) | 8.00 cm$^{-1}$ |

B. Intensity Measurements

| | |
|---|---|
| Diffractometer | Rigaku AFC6S |
| Radiation | MoKα ($\lambda$ = 0.71069 Å) |
| | graphite monochromated |
| Take-off Angle | 6.0° |
| Detector Aperture | 4.0 mm horizontal |
| | 4.0 mm vertical |
| Crystal to Detector Distance | 200 mm |
| Temperature | 23.0°C |
| Scan Type | ω-2θ |
| Scan Rate | 2.0°/min (in ω) (up to 4 scans) |
| Scan Width | (1.20 + 0.34 tan θ)° |
| $2THETA_{max}$ | 50.1° |
| No. of Reflections Measured | Total: 4980 |
| Corrections | Lorentz-polarization<br>Absorption<br>(trans. factors: 0.7896 - 1.0000)<br>Secondary Extinction<br>(coefficient: 4.38672e-08) |

C. Structure Solution and Refinement

| | |
|---|---|
| Structure Solution | Patterson Methods (DIRDIF92 PATTY) |
| Refinement | Full-matrix least-squares |
| Function Minimized | $\sigma$ w (\|Fo\| - \|Fc\|)$^2$ |
| Least Squares Weights | $1/^2\sigma(Fo) = 4Fo^2/\sigma^2(Fo^2)$ |
| p-factor | 0.0200 |
| Anomalous Dispersion | All non-hydrogen atoms |
| No. Observations (I>3.00sigma(I)) | 3238 |
| No. Variables | 224 |
| Reflection/Parameter Ratio | 14.46 |
| Residuals: R; Rw | 0.032 ; 0.037 |
| Goodness of Fit Indicator | 2.05 |
| Max Shift/Error in Final Cycle | 0.02 |
| Maximum peak in Final Diff. Map | 0.61 $e^-/Å^3$ |
| Minimum peak in Final Diff. Map | -0.34 $e^-/Å^3$ |